syndromes: progress over the past decade. Muscle Nerve 2003; 27: 4-25.
19) 福留隆泰.〔神経筋接合部疾患の病態へのアプローチ〕先天性筋無力症候群の診断と病態へのアプローチ. 臨床脳波(0485-1447)2002; (44) 9: 562-5.
20) Kohara N, Lin TS, Fukudome T, et al. Pathophysiology of weakness in a patient with congenital endplate acetylcholinesterase deficiency. Muscle Nerve 2002; 25: 585-92.

THE JOURNAL OF BIOLOGICAL CHEMISTRY
Vol. 279, No. 11, Issue of March 12, pp. 10286–10292, 2004
Printed in U.S.A.

Laminin α2 Is Essential for Odontoblast Differentiation Regulating Dentin Sialoprotein Expression*

Received for publication, September 9, 2003, and in revised form, December 1, 2003
Published, JBC Papers in Press, December 16, 2003, DOI 10.1074/jbc.M310013200

Kenji Yuasa‡§¶, Satoshi Fukumoto‡¶‖, Yoko Kamasaki‡, Aya Yamada‡, Emiko Fukumoto, Kazuhiro Kanaoka§, Kan Saito‡, Hidemitsu Harada‡‡, Eri Arikawa-Hirasawa§§, Yuko Miyagoe-Suzuki¶¶, Shinichi Takeda¶¶, Kuniaki Okamoto§, Yuzo Kato§, and Taku Fujiwara‡**

*From the ‡Division of Pediatric Dentistry and §Oral Molecular Pharmacology, Department of Developmental and Reconstructive Medicine, and **Division of Oral Health Services Research, Department of Public Health, Nagasaki University Graduate School of Biomedical Sciences, 1-7-1 Sakamoto, Nagasaki 852-8588, ‡‡Department of Oral Anatomy and Developmental Biology, Osaka University Graduate School of Dentistry, 1-8 Yamadaoka, Suita, Osaka 565-0871, the §§Department of Neurology, Juntendo University School of Medicine, 2-1-1 Hongo, Bunkyo-ku, 113-8421 Tokyo, and the ¶¶Department of Molecular Therapy, National Institute of Neuroscience, National Center of Neurology and Psychiatry, 4-1-1 Ogawa-higashi, Kodaira, Tokyo 187-8502, Japan*

Laminin α2 is subunit of laminin-2 (α2β1γ1), which is a major component of the muscle basement membrane. Although the laminin α2 chain is expressed in the early stage of dental mesenchyme development and localized in the tooth germ basement membrane, its expression pattern in the late stage of tooth germ development and molecular roles are not clearly understood. We analyzed the role of laminin α2 in tooth development by using targeted mice with a disrupted *lama2* gene. Laminin α2 is expressed in dental mesenchymal cells, especially in odontoblasts and during the maturation stage of ameloblasts, but not in the pre-secretory or secretory stages of ameloblasts. *Lama2* mutant mice have thin dentin and a widely opened dentinal tube, as compared with wild-type and heterozygote mice, which is similar to the phenotype of dentinogenesis imperfecta. During dentin formation, the expression of dentin sialoprotein, a marker of odontoblast differentiation, was found to be decreased in odontoblasts from mutant mice. Furthermore, in primary cultures of dental mesenchymal cells, dentin matrix protein, and dentin sialophosphoprotein, mRNA expression was increased in laminin-2 coated dishes but not in those coated with other matrices, fibronectin, or type I collagen. Our results suggest that laminin α2 is essential for odontoblast differentiation and regulates the expression of dentin matrix proteins.

Tooth development is regulated by sequential and reciprocal interactions between neural crest-derived mesenchymal cells and the oral environment (1–3); however, the precise molecular mechanisms mediating interactions between epithelium and mesenchymal cells are not clear, although basement membrane (BM)[1] components have been shown to play important roles in these regulatory events. In addition, the extracellular matrix layer, whose main components are laminin, collagen IV, nidogen, and sulfated proteoglycan, and the BM layer are both considered to be involved with cell proliferation and differentiation (4, 5).

The laminin family is composed of BM proteins that have been implicated in diverse functions of epithelial and mesenchymal cells. Each member is a heterotrimer composed of α, β, and γ chains, and five α, three β, and three γ chains have been identified and are known to form at least 15 heterotrimer structures. Most laminin family members have been found to have combinations of β1γ1 or β2γ1 chains with one of the five α chains, although laminin-5 has a unique chain composition, α3β3γ2.

Laminin-2 (with α2, β1, and γ1 chains), also known as merosin, is a major component of BM proteins in skeletal muscle and the peripheral nervous system (6), and the absence of the laminin α2 chain causes merosin-deficient congenital muscular dystrophy (MD-CMD) (7), which characteristically involves skeletal muscle along with the peripheral and central nervous systems (8). MD-CMD causes degradation, regeneration, interstitial fibrosis, and adipose tissue infiltration in skeletal muscle. Dystrophic (dy/dy) mice also display a severe reduction in laminin α2 chain expression and are accepted as an animal model of MD-CMD (6, 9–11). We generated a null mutant lacking the laminin α2 chain using a gene-targeting technique to examine the molecular pathophysiology of MD-CMD (12). The mice showed symptoms similar to those seen in MD-CMD and a shorter life span than dy/dy mice (13).

During tooth development, the mRNA of three laminin α chains, α1, α2, and α4, is expressed in tooth mesenchymal cells, whereas two other types, laminin α3 and α5 chain mRNA, are found in epithelial cells (14, 15). Furthermore, laminin α5 mRNA is widely expressed in tooth epithelium, with the corresponding protein distributed along the tooth basement membrane during the embryonic stage and diminished at the start of enamel matrix production (14). Laminin α3 expression is slight in the embryonic stage and then dramatically increases during terminal differentiation of ameloblasts, following degradation of the tooth BM (14, 16). On the other hand, laminin

* This work was supported by Grants-in-aid for Scientific Research in a Priority Area 15689025 and 15791255 from the Ministry of Education, Science, Sports and Culture of Japan. The costs of publication of this article were defrayed in part by the payment of page charges. This article must therefore be hereby marked "*advertisement*" in accordance with 18 U.S.C. Section 1734 solely to indicate this fact.

¶ *Both authors contributed equally to this work.*

‖ To whom correspondence should be addressed: Division of Pediatric Dentistry, Dept. of Developmental and Reconstructive Medicine, Nagasaki University Graduate School of Biomedical Sciences, 1-7-1 Sakamoto, Nagasaki 852-8588, Japan. Tel.: 81-95-849-7674; Fax: 81-95-849-7675; *E-mail: satoshi@dh.nagasaki-u.ac.jp.*

[1] The abbreviations used are: BM, basement membrane; DSP, dentin sialoprotein; DMP, dentin matrix protein; MD-CMD, merosin-deficient congenital muscular dystrophy; DSPP, dentin sialophosphoprotein; AMBN, ameloblastin; AMEL, amelogenin; PBS, phosphate-buffered saline; RT, reverse transcription/transcriptase; G3PDH, glyceraldehydes-3-phosphate dehydrogenase; AI, amelogenesis imperfecta; ANOVA, analysis of variance; SEM, scanning electron microscope; LG, laminin-type G.

α2 mRNA is detected in mesenchymal cells in the tooth germ. In the earlier stages, mesenchymal expression is seen around the epithelial bud, while in later stages (E15–18) laminin α2 mRNA expression becomes stronger in dental sac cells than in dental papilla cells. By using immunohistostaining, laminin α2 can be detected in the tooth germ BM before E15, although later (E15–18) staining is lost from the dental BM, the area between the inner dental epithelium and dental papilla mesenchyme layers, whereas it remains strong in the BM area between the outer dental epithelium and dental sac mesenchyme (14). However, the expression and molecular mechanisms of laminin α2 in postnatal tooth development have not been clearly shown.

In the present study, we examined tooth formation and dentin sialoprotein (DSP) expression in laminin α2 knockout mice, a mutant strain with thin enamel and a widely opened dentinal tube, which are caused by a reduction of dentin formation and odontoblast differentiation. Laminin-2 enhances the expression of dentin sialophosphoprotein (DSPP) and dentin matrix protein (DMP) in primary cultured dental mesenchymal cells. Our present findings suggest that interactions between laminin α2 and odontoblasts regulate their differentiation and are important for dentinogenesis.

EXPERIMENTAL PROCEDURES

Scanning Electron Microscope (SEM) Analysis—Incisors were taken from wild-type and laminin α2 null mice and coated with gold and photographed using scanning electron microscopy at 20 kV (S-3500, Hitachi Ltd., Tokyo, Japan). To observe the enamel crystals and dentinal tubes, the specimens were embedded in epoxy resin, cut with an ISOMET low speed saw (Buehler, Lake Bluff, IL), and then treated with 40% phosphoric acid for 10 s and 10% sodium hypochlorite for 30 s, prior to coating with gold.

Preparation of Tissue Sections—Laminin α2 null mice were generated by gene targeting and housed in a pathogen-free animal facility. Standard Nagasaki University guidelines were followed to monitor their health status as well as the housing and breeding practices. To prepare the heads of 3-week-old mice, each animal was anesthetized and then fixed by perfusion with 4% paraformaldehyde/PBS. The maxilla was dissected out, post-fixed overnight at 4 °C in 4% paraformaldehyde/PBS, and decalcified with 250 mM EDTA/PBS for 2 weeks, then dehydrated in xylene through a graded ethanol series, and embedded in paraplastic paraffin (Oxford Laboratories). Sections were cut at 10 μm on a microtome (RM2155, LEICA, Inc.). For detailed morphological analyses of molars and incisors, sections were stained with Harris hematoxylin and eosin Y (Sigma). For staining of cultured cells, cells were fixed with 4% paraformaldehyde, 0.5% Triton X-100, PBS for 5 min and then 4% paraformaldehyde/PBS for 10 min.

Immunolistochemistry—Immunohistochemistry was performed on the sections, which were incubated in 1% bovine serum albumin/PBS as a blocking agent for 1 h prior to incubation with primary antibodies. We used antibodies directed against laminin α2 (4H8–2, Alexis) (12), ameloblastin (AMBN) (17), amelogenin (AMEL) (18, 19), and DSP (20) (provided by Yoshihiko Yamada). The primary antibodies were detected using fluorescein isothiocyanate or Cy-3-conjugated secondary antibodies (Jackson ImmunoResearch).

Dental Epithelial and Mesenchymal Cell Cultures—For dental mesenchymal cell cultures, P3 mouse molars were dissected and treated with 0.1% collagenase, 0.05% trypsin, 0.5 mM EDTA for 10 min, after which the dental mesenchyme was separated from the dental epithelium. Separated dental mesenchyme samples were treated with 0.1% collagenase, 0.05% trypsin, 0.5 mM EDTA for 15 min and then collected using a pipette and placed into the wells (21). Dental mesenchymal cells were cultured in Dulbecco's modified Eagle's medium (Invitrogen) with 10% fetal calf serum, whereas a dental epithelial cell line (HAT-7) was cultured in Dulbecco's modified Eagle's medium/F-12 with 10% fetal calf serum (22).

RNA Isolation and RT-PCR—Developing molars were dissected from P3 mice, and RNA was isolated using TRIzol reagent, according to the manufacturer's instructions (Invitrogen). First strand cDNA was synthesized at 42 °C for 90 min using oligo(dT)$_{14}$ primer. Real time PCR amplification was performed using primers for AMBN (5′-GCGTTTCCAAGAGCCCTGATAAC-3′ and 5′-AAGAAGCAGTGTCACATTTCCTGG-3′), AMEL (5′-ATTCCACCCCAGTCTCATCAG-3′ and 5′-CCACTTCGGTTCTCTCATTTTCTG-3′), enamelin (5′-GTGAGGAAAAATACTCCATATTCTGG-3′ and 5′-GTTGAAGCGATCCCTAAGCCTGAAGCAG-3′), enamelysin (MMP-20) (5′-AGATGGTGGCAAGAGAA-3′ and 5′-GAGATTCCGTATGTCAAAAT-3′), DSPP (5′-CTCAGAGAGAATCTGGGTGTACCACC-3′ and 5′-CACAGTGGTACATGGAGAGCTC-3′), DMP (5′-GCTTCAGGCTCAGTCTTGCT-3′ and 5′-TGTAACCCTCCAACTCCAGG-3′), osteonectin (5′-GTCTCACTGGCTGTGTTGGA-3′ and 5′-AAGACTTGCCATGTGGGTTC-3′), osteopontin (5′-CGATGATGATGACGATGGAG-3′ and 5′-GAGGTCCTCATCTGTGGCAT-3′), osteocalcin (5′-CCTCTTGAAAGAGTGGGCTG-3′ and 5′-CCTCGGGAGACAAACAACAT-3′), and G3PDH (5′-CCATCACCATCTTCCAGGAG-3′ and 5′-GCATGGACTGTGGTCATGAG-3′), with SYBR Green PCR Master Mix by TaqMan 7700 Sequencer Detection (Applied Biosystems). PCR was performed for 40 cycles, 95 °C for 1 min, 58 °C for 1 min, and 72 °C for 1 min as reported previously (21).

Cell Proliferation and Cell Binding—Dental epithelial cells (HAT-7) and dental mesenchymal cells at 1.0×10^5 were cultured in a 60-mm diameter dish coated with or without laminin-2 (merosin, Invitrogen), type I collagen (Cellmatrix, NITTA GERATIN, Japan), and fibronectin (human fibronectin, Invitrogen) for 5 days. At 1, 3, and 5 days after plating, cells were treated with 0.05% trypsin, 0.5 mM EDTA, and their numbers were counted under a microscope. For cell binding, dental epithelial and mesenchymal cells were detached with 0.05% EDTA, washed with Dulbecco's modified Eagle's medium containing 0.1% bovine serum albumin, and resuspended to a concentration of 3.5×10^6/ml. Assays were performed in 96-well round-bottomed microtiter plates (Immulon-2HB, Dynex Technologies, Inc., Chantilly, VA). Wells were coated overnight at 4 °C with laminin 2, type I collagen, or fibronectin, then diluted with PBS, and blocked with 3% bovine serum albumin for 1 h at 37 °C. After washing, the cells were added to a plate and incubated for 60 min at 37 °C. Attached cells were stained for 10 min with 0.2% crystal violet (Sigma) in 20% methanol. After washing with H_2O, the cells were dissolved in 10% SDS, and absorbance at 600 nm was measured.

RESULTS

Laminin α2 Expression in Differentiated Odontoblasts and Maturation of Ameloblasts—Laminin α2 is known to be expressed in dental mesenchymal cells and localizes in the BM area between the dental epithelium and mesenchyme layers in the early stage of tooth germ development (14); however, its expression in later stages, especially in the postnatal period, has not been clearly identified. We performed immunostaining of incisor samples from 3-week-old mice to identify the localization of laminin α2, which was found expressed in the preameloblast and pre-odontoblast interfaces (Fig. 1*A*, *a*), as well as in odontoblasts, the outer side of the dental epithelium including the papillary cell layer, capillaries, and the muscle BM (Fig. 1*A*, *a* and *b*). However, laminin α2 expression was not observed in the cervical loop region or the secretory stage of ameloblasts (Fig. 1*B*, *a*). Later, in the early maturation (Fig. 1*B*, *b*) and late maturation (Fig. 1*B*, *c*) stages, laminin α2 appeared in the side of the enamel. On the other hand, laminin α2 expression was detected in odontoblasts at all stages (Fig. 1*C*). To confirm the expression in odontoblasts, immunostaining of primary cultured dental mesenchymal cells was performed, and laminin α2-positive cells were found expressed in DSP (Fig. 1*D*), which is a marker of odontoblasts, indicating that the odontoblasts produced laminin α2.

Decreased Dentin Formation and Amelogenesis Imperfecta in Laminin α2 Null Mice—For the targeted disruption of LAMA2, a PGK-neo gene was inserted into the laminin α2 chain (12). These mice had been back-crossed into the BALB/c strain at least 10 times, before the tooth phenotype was analyzed. To examine laminin α2 expression in the masseter muscle, we performed immunostaining of 3-week-old wild-type, heterozygous, and null mutant mice, using rat anti-laminin α2 chain monoclonal antibody 4H8–2, which recognizes the 300-kDa portion of the protein (23). The results confirmed the absence of the laminin α2 chain in mutant strain muscles. Laminin α2-positive staining was observed in the muscle BM (Fig. 2*A*, *a* and *b*) in the wild-type and heterozygote mice but not in the

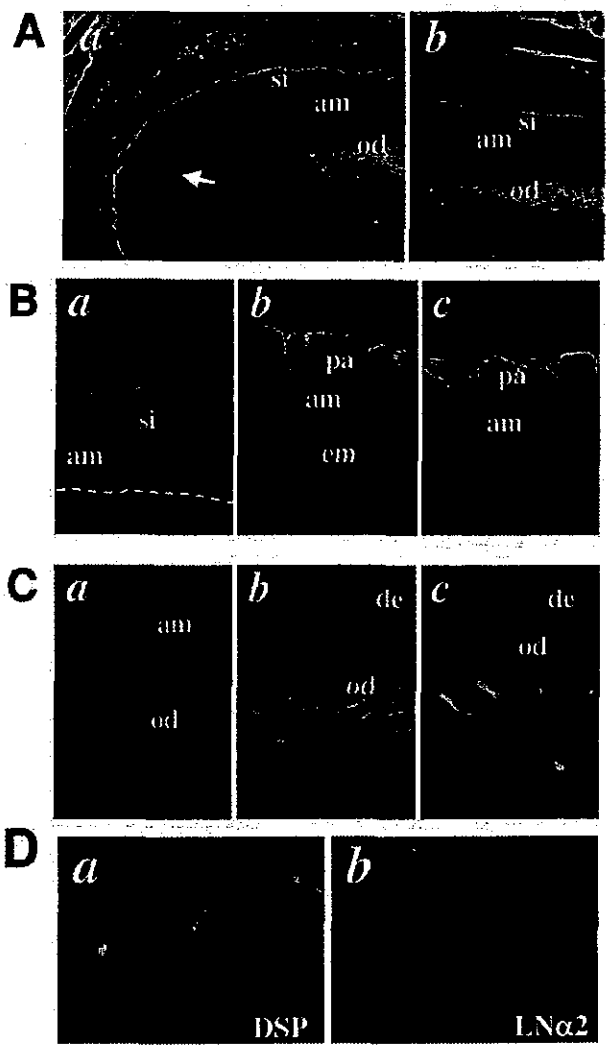

FIG. 1. **Laminin α2 expression in incisor ameloblasts and odontoblasts.** *A*, 3-week-old mice incisor cells were immunostained with anti-laminin α2 antibody as described under "Experimental Procedures." *a*, laminin α2 expression was found in the pre-ameloblast and odontoblast interface (*arrow*), and it continued in the secretory stage (*b*). *B*, higher magnification of incisor ameloblasts in each stage. Laminin α2 expression was not observed in secretory stage ameloblasts (*a*). Later, in the early maturation (*b*) and late maturation (*c*) stages, laminin α2 appeared in the side of the enamel. It was also detected in the outer side of the dental epithelium as well as the papillary cell layer in all stages. *C*, higher magnification of incisor odontoblasts in each stage corresponding to the ameloblast developmental stages as shown in *B*. Laminin α2 expression was detected in odontoblasts at all stages (*a–c*). *D*, primary cultured dental epithelial cells were stained with anti-DSP (*a*) and laminin α2 (*b*) antibodies. *si*, stratum intermedium; *pa*, papillary cell layer; *am*, ameloblast; *od*, odontoblast; *em*, enamel matrix; *de*, dentin.

mutants (Fig. 2*A*, *c*). In the same mice used to analyze laminin α2 expression in the masseter muscle, the color of the incisor surface in the mutants was found to be white when compared with the wild-type and heterozygote mice, indicating amelogenesis imperfecta (AI) (Fig. 2*B*). For detailed analyses of the incisor enamel and dentin, scanning microscopic examinations were performed. The overall tooth length and shape of the upper incisors were not different between the heterozygote and mutant mice (Fig. 2*C*); however, the cross-sectional surface of the incisor was decreased, as well as the enamel and dentin thickness by ~13 and 25%, respectively, in the mutant specimens (Fig. 2, *D* and *E*). Furthermore, the surface of the superficial enamel was rough as compared with that of the heterozygote incisors, resulting in the white color (Fig. 3*d*). In contrast, the size and structure of the enamel were not different between the two types of mice. On the other hand, the dentinal tubes were opened wide in the mutant mice following treatment with phosphoric acid and sodium hypochlorite, indicating immature dentin in the surrounding area (Fig. 3*e*). In the SEM analysis, enamel surface and dentin structures were not different between the wild-type and heterozygote mice (data not shown).

Decreased Expression of DSP in Laminin α2 Null Mice—To analyze the differentiation of ameloblasts and odontoblasts in mutant mice, we performed immunohistochemistry examinations using antibodies to AMEL, AMBN, and DSP. The AMEL and AMBN expression patterns during the secretory stage of ameloblasts were not altered in mutant incisors as compared with those from the wild-type and heterozygote mice (Fig. 4*A*). Furthermore, by using hematoxylin and eosin staining of dentin and odontoblasts, the width of the predentin and shape of odontoblasts in laminin α2 null mice were shown not to be different from those of the wild-type and heterozygote mice. However, DSP expression in odontoblasts was dramatically reduced in the mutant mice teeth (Fig. 4*B*). In addition, DMP, DSPP, and osteopontin mRNA expressions in dissected incisors were also decreased in two of the mutant mice (Fig. 5), whereas DMP, DSPP, and osteopontin mRNA were highly expressed in those from the wild type. DMP mRNA expression in two mutant strains was dramatically decreased by ~60%, whereas DSP and osteopontin mRNA were decreased by ~70% (Fig. 5). These results suggest that the differentiation of odontoblasts in the mutant mice was inhibited by the absence of the laminin α2 chain.

Laminin-2 Inhibits the Expression of Enamel Matrix and Enhances Dentin Matrix Proteins—BM components in ameloblasts, including laminin and collagen IV, are known to disappear in the secretory stage and reappear in the maturation stage (14, 24, 25). In the present study, laminin α2 showed an expression pattern similar to other BM proteins (Fig. 1). To analyze the effect of laminin-2 on ameloblasts, a rat dental epithelial cell line (HAT-7) was cultured in several extracellular matrix-coated dishes for 3 days, after which marker gene expression was analyzed by RT-PCR. In HAT-7 cells, AMEL expression was inhibited by laminin 2, fibronectin, and type I collagen (Fig. 6*A*). Furthermore, enamelin and MMP-20 (enamelysin) expression was also decreased in those matrix cultures (Fig. 6*A*), whereas AMBN expression in HAT-7 was not detected under any of the tested conditions (data not shown). These results suggest that laminin-2 inhibits ameloblast differentiation in the secretory stage. Laminin α2 is known to be expressed in dental mesenchymal cells in the early stage and then transiently disappears in mesenchymal cells facing the inner dental epithelium. In the present study, this expression reappeared and continued during dentin formation. To identify the role of laminin α2 with odontoblast differentiation, dental mesenchymal cells from P3 molar tooth germ samples were cultured in laminin-2, fibronectin, and type I collagen-coated dishes, and ~15% of the cells were found to be DSP-positive by immunostaining (data not shown). Furthermore, the expression of DSPP and DMP was increased 3–4-fold in the laminin-2-coated dish, whereas there were no changes in those coated with fibronectin or type I collagen (Fig. 6*B*).

No Effect by Laminin-2 on Proliferation and Cell Binding of Dental Mesenchymal Cells—In general, the extracellular matrix is important for proliferation and differentiation of dental epithelium and mesenchymal cells. However, long term cultures of dental epithelial cells was shown to lead to an enhance-

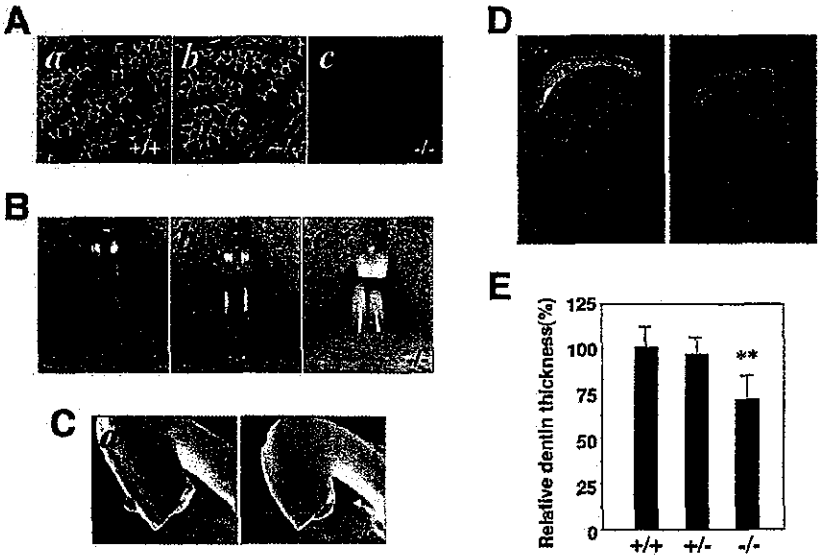

FIG. 2. **Tooth abnormalities in 3-week-old lama2−/− mice.** *A*, immunostaining with laminin α2 in masseter muscle tissues from wild-type (*a*), heterozygote (*b*), and mutant (*c*) mice. *B*, the color of the mutant incisor surfaces was white (*c*) as compared with the wild-type (*a*) and heterozygote (*b*) mice. *C*, overall tooth shape was not different between the heterozygotes (*a*) and mutants (*b*) in the SEM analysis. *D*, dentin thickness in the incisor cross-sectional surface area was decreased in the mutant (*b*) as compared with the heterozygote (*a*) mice in the SEM analysis. *E*, dentin thickness in the wild-type and heterozygote mice was not different, but dentin width in the mutants was decreased ~25%. Statistical analysis was performed using ANOVA (**, $p < 0.05$).

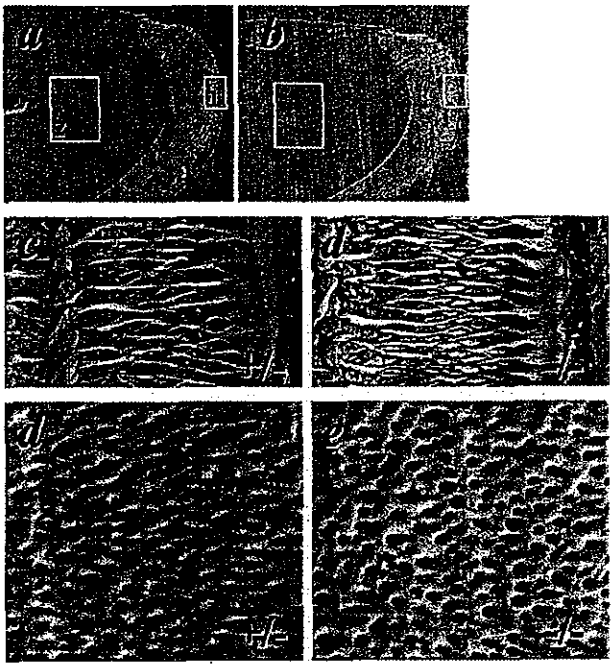

FIG. 3. **Rough surface of superficial enamel and widely opened dentinal tubes in lama2−/− mice.** SEM analysis of the incisor specimens from heterozygote (*a*, *c*, and *d*) and mutant (*b*, *d*, and *e*) mice was performed as described under "Experimental Procedures." Higher magnified images of superficial enamel (*c* and *d*) and dentinal tubes (*d* and *e*) in the *boxed region* of *a* and *b* are also shown. The superficial enamel of the mutant incisors was rough (*d*) as compared with that from the heterozygotes (*c*). The dentinal tubes were opened wide in the mutant specimens (*e*) following treatment with phosphoric acid and sodium hypochlorite.

ment of cell proliferation and decrease of the enamel matrix protein amelogenin in collagen-coated dishes (26). To determine whether the decrease of amelogenin and increase of DMP and DSPP mRNA in laminin-2-coated dishes was dependent on cell proliferation, we analyzed the effect of matrices on cell proliferation (Fig. 7). Cells were cultured with each matrix, and their numbers were counted after 5 days. HAT-7 proliferation in the type I collagen dish was increased (Fig. 7*A*), but not in the laminin-2 or fibronectin dishes, with similar results observed in the primary cultured dental mesenchymal cells (Fig. 7*B*). Type I collagen coating is known to have a greater effect on the expression of enamel matrix proteins than laminin-2 and fibronectin. Our results suggest that the decrease of enamel matrix expression in the type I collagen-coated dish may have been caused by an increase of cell proliferation. However, the decrease of amelogenin seen in dental epithelial cells and the increase of DMP and DSPP mRNA seen in dental mesenchymal cells cultured with laminin-2 may not have been dependent on cell proliferation.

Laminin is associated with several extracellular matrix and cell receptors that are important for cell binding. We hypothesized that laminin-2 directly binds to dental epithelial and mesenchymal cells and regulates the gene expression of dentin and enamel matrices. To analyze the cell binding activity of laminin-2, cells were incubated in laminin-2-coated microtiter plates as described under the "Experimental Procedures" (Fig. 8). We found that dental epithelial cell binding to laminin-2 was significantly weaker than that to fibronectin and type I collagen (Fig. 8*A*), whereas dental mesenchymal cells showed little or no binding to the laminin-2-coated plate (Fig. 8*B*).

DISCUSSION

This is the first known analysis of laminin α2 expression in differentiated ameloblasts and odontoblasts during odontogenesis and tooth development in mutant mice. Laminin α2 chain mRNA and protein are expressed in several organs besides striated muscles, including the central nervous system (6), thyroid gland, thymus, kidney, testis, skin, and digestive tract. In addition, laminin α2 is also expressed in the tooth germ during amelogenesis and dentinogenesis in a stage-specific manner (14). In the present study, laminin α2 chain mRNA was found intensely expressed in dental sac cells. Furthermore, results from immunostaining for laminin α2 expression were in conformity with the detected mRNA patterns, indicating a role for the laminin α2 chain in the production of BM proteins by dental mesenchymal cells. Salmivirta *et al.* (14) reported that no laminin α chains (α1, α2, and α4) expressed by mesenchymal cells were found in secretory odontoblasts. However, they analyzed molars from embryonic stage and postnatal day 1 mice, during which odontoblasts are partially differentiated. For this reason, we used incisors from 3-week-old mice to investigate the expression of laminin α2 chain in fully differentiated ameloblasts and odontoblasts. The BM of the cervical

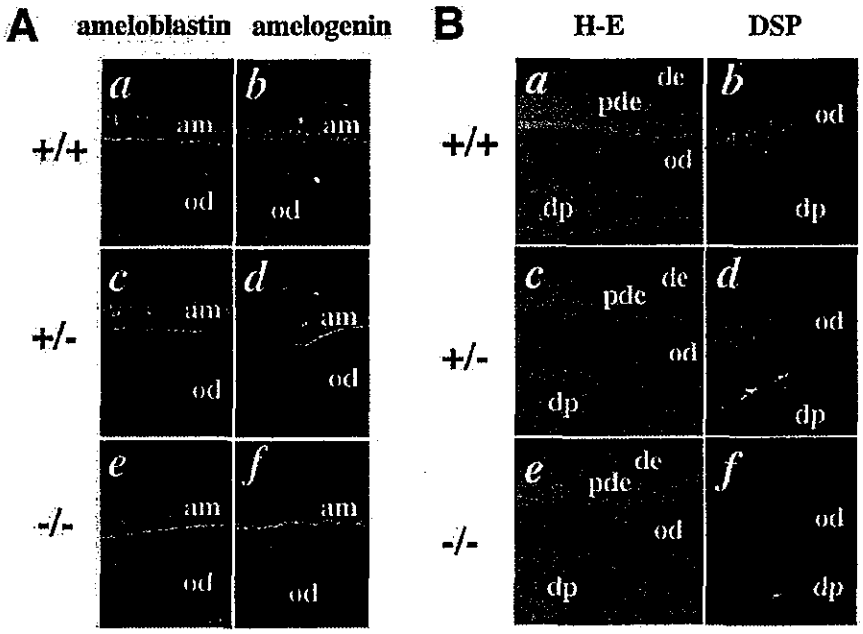

FIG. 4. **Decreased expression of DSP in lama2−/− mice.** *A*, immunostaining with anti-ameloblastin (*a*, *c*, and *e*) and amelogenin (*b*, *d*, and *f*) antibodies in secretory stage ameloblasts from wild-type (*a* and *b*), heterozygote (*c* and *d*), and mutant (*e* and *f*) mice. Ameloblastin and amelogenin expressions were not different. *B*, hematoxylin and eosin staining (*a*, *c*, and *e*) and immunostaining with anti-DSP antibody (*b*, *d*, and *f*) in differentiated odontoblasts from wild-type (*a* and *b*), heterozygote (*c* and *d*), and mutant (*e* and *f*) mice. The width of the predentin and shape of the odontoblasts in the mutants (*e*) were not different from the wild-type (*a*) or heterozygote mice (*c*). DSP expression was dramatically decreased in mutant odontoblasts (*f*). *am*, ameloblast; *od*, odontoblast; *de*, dentin; *pde*, predentin; *dp*, dental pulp.

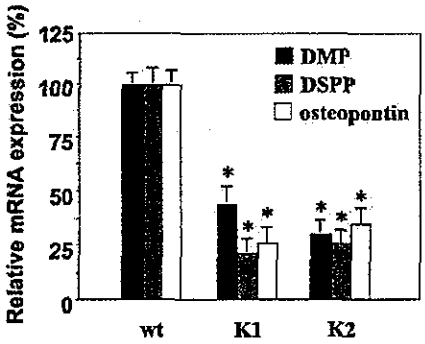

FIG. 5. **Decreased expression of DMP, DSPP, and osteopontin mRNA in lama2−/− mice.** Incisors were dissected from the maxillas of wild type (*wt*) and two mutant (K1 and K2) strains of 3-week-old mice, and then mRNA was isolated and amplified using quantitative RT-PCR, real time PCR, methods with specific primer sets as described under "Experimental Procedures." The expressions of DMP, DSPP, and osteopontin mRNA were decreased in both mutant strains. G3PDH mRNA was used as the control. G3PDH expression was not different between each sample (data not shown). mRNA expression in the mutant samples was compared with that in the wild type. Statistical analysis was performed using ANOVA (*, $p < 0.01$).

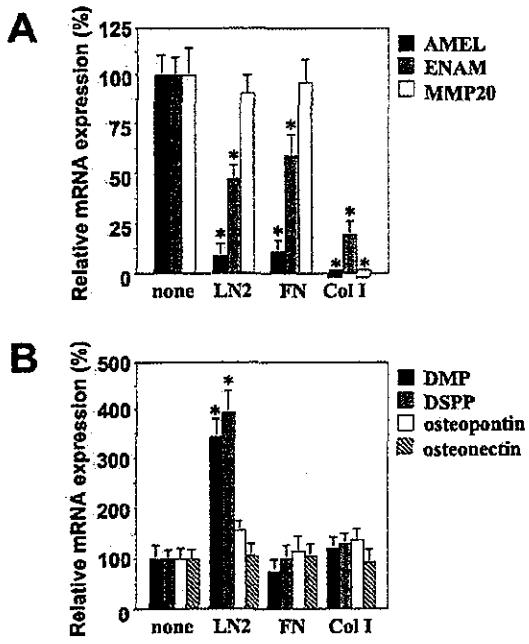

FIG. 6. **Laminin-2 inhibits the expression of enamel matrix and enhances dentin matrix proteins.** A dental epithelial cell line (HAT-7) (*A*) and primary dental mesenchymal cells (*B*) were cultured in dishes coated with or without laminin-2, fibronectin, or type I collagen for 2 days. mRNA was isolated and amplified using a quantitative RT-PCR method with specific primer sets as described under "Experimental Procedures." AMEL and enamelin (*ENAM*) expression were decreased in dental epithelial cells in laminin-2, fibronectin, and type I collagen-coated dishes. DMP and DSPP expression were increased in dental mesenchymal cells cultured in laminin-2-coated dishes. G3PDH mRNA was used as the control. G3PDH expression was not different between each sample (data not shown). These experiments were repeated at least three times with similar results. mRNA expressions in each matrix in HAT-7 and in primary cultured dental mesenchymal cells were compared with non-coated dishes. Statistical analysis was performed using ANOVA (*, $p < 0.01$).

loop in the incisor did not express the laminin α2 chain, indicating that there is no expression in inner dental epithelium or dental mesenchymal cells in molars. In contrast, expression was observed in the interface between pre-ameloblasts and odontoblasts, whereas laminin α2 transiently disappeared during odontoblast differentiation.

Because dy^{3K}/dy^{3K} mice have no laminin α2 chain, they are excellently suited for analysis of the biological functions of the laminin α2 chain in various organs (12). In the present study, we analyzed laminin α2 null mutant mice in order to identify the role of laminin α2 in the tooth development. These mice showed irregular enamel surface structures and a decrease of dentin formation, whereas ameloblasts expressed the laminin α2 chain in the maturation stage but not in the secretory stage (Fig. 1). Furthermore, enamel abnormalities were only observed in superficial enamel, because of the restriction of laminin α2 chain expression, resulting in white colored incisors. However, the structure and size of the enamel crystals were not different between heterozygote and mutant mice, because there was no laminin α2 expression in secretory stage ameloblasts.

Amelogenin and ameloblastin, tooth-specific extracellular

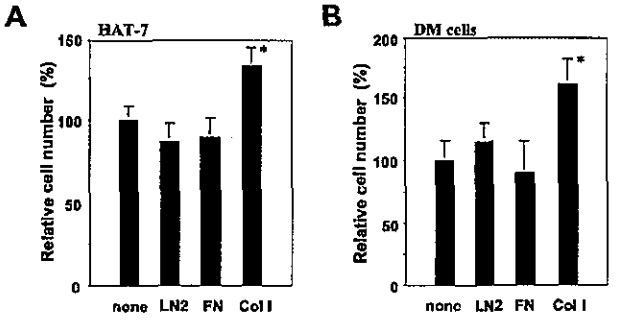

FIG. 7. **Proliferation of HAT-7 and primary dental mesenchymal cells in laminin-2, fibronectin, and type I collagen-coated dishes.** A dental epithelial cell line (HAT-7) (*A*) and primary dental mesenchymal cells (*B*) were cultured in dishes coated with or without laminin-2 (*LN2*), fibronectin (*FN*), or type I collagen (*Col I*) for 5 days. Cells were prepared and counted as described under "Experimental Procedures." Laminin-2 coating did not affect the proliferation of HAT-7 and primary dental mesenchymal cells. Type I collagen coating enhanced cell proliferation by both types of cells. These experiments were repeated at least three times with similar results. Cell proliferation in each matrix in HAT-7 and in primary cultured dental mesenchymal cells was compared with non-coated dishes. Statistical analysis was performed using ANOVA (*, $p < 0.01$).

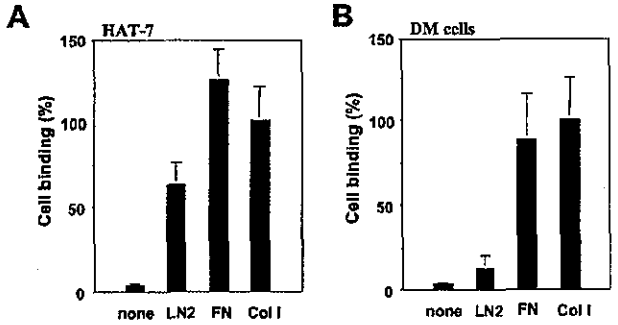

FIG. 8. **Binding of HAT-7 and primary dental mesenchymal cells to laminin-2, fibronectin, and type I collagen.** A dental epithelial cell line (HAT-7) (*A*) and primary dental mesenchymal cells (*B*) were cultured and plated on microtiter plates coated with laminin-2, fibronectin, or type I collagen. *A*, cell binding activity was analyzed as described under "Experimental Procedures." HAT-7 cells bound to laminin-2, although the binding activity was lower than to fibronectin and type I collagen. *B*, dental mesenchymal cells showed little or no binding to laminin-2-coated plates.

matrix proteins, are specifically expressed in secretory ameloblasts (17, 27–30). In patients, numerous mutations have been found in amelogenin coding sequences, with the most common genetic disorder, AI, affecting enamel (31–33). In another study, targeted disruption of the amelogenin gene locus in mice caused a hypoplastic enamel phenotype similar to AI, confirming the important role of amelogenin in enamel formation (34). Ameloblastin is also thought to have a relationship with the autosomal dominant type of AI (35). In the present laminin α2 null mutants, the expression of these enamel matrix proteins was not changed, indicating that ameloblast differentiation in the secretory stage was undisturbed, because there was no expression of laminin α2 found. Furthermore, other BM components, including collagen IV and, notably, BM proteins, were not expressed in secretory stage ameloblasts and reappeared in the maturation stage, indicating that ameloblasts may adhere to enamel surfaces via an extracellular matrix. In fact, laminin-2 was shown to have cell binding activity identical to a dental epithelial cell line, HAT-7, and did not affect cell proliferation in either HAT-7 cells or primary cultured dental mesenchymal cells.

In odontoblasts, laminin α2 expression continued during dentinogenesis. A decrease in dentin width and the occurrence of clearly opened dentinal tubes were phenotypic changes more severe than those seen in the enamel, as biomineralization of the dentin extracellular matrix requires complex interactions among several collagenous and non-collagenous molecules. Surprisingly, the expressions of Dspp mRNA and DSP protein were decreased in laminin α2 mutant odontoblasts, as Dspp was primarily found expressed by odontoblasts and pre-ameloblasts. Dspp mRNA is translated into a single protein, Dspp, and cleaved into two peptides, dentin DSP and dentin phosphoprotein (DPP), which become localized within the dentin matrix (36–40). Furthermore, the expression pattern of Dspp in odontoblasts is similar to that of laminin α2. Recently, mutations in this gene were identified in human dentinogenesis imperfecta II (Online Mendelian Inheritance in Man accession number 125490) and dentin dysplasia II (Online Mendelian Inheritance in Man accession number 125420) syndromes (41, 42). Dspp-null mice were also generated and found to develop tooth defects similar to human dentinogenesis imperfecta III with enlarged pulp chambers, an increased predentin zone width, hypomineralization, and pulp exposure (43). Interestingly, the levels of biglycan and decorin, small leucine-rich proteoglycans, were increased in the widened predentin zone and in void spaces among the calcospherites in the dentin of those null mice. Decorin also functions as an inhibitor of mineralization during primary ossification of mouse embryo bones (44), whereas biglycan facilitates the initiation of apatite formation and inhibits the growth of apatite (45). These results suggest that Dspp is essential for dentin mineralization, including the potential regulation of proteoglycan levels, and is involved in the results of the present study, as the expression of DSP and DMP was decreased in the incisors of laminin α2 null mice, indicating an inhibition of odontoblast differentiation. Similar results were observed in primary cultured dental mesenchymal cells.

It was recently reported that a lack of the laminin α2 chain results in apoptosis of myogenic cells *in vitro*, as this chain appears to promote myotube stability by preventing cell death (46). Similar results were observed in the muscle tissue cells of the present laminin α2 mutant mice, as there was a markedly high number of apoptotic nuclei that were terminal dUTP nick-end labeling-positive, as compared with wild-type littermates (12). However, in the tooth germ specimens, apoptosis was not observed in ameloblasts or odontoblasts (data not shown), and no changes in the numbers or morphology of these cells were detected. These results suggest that a reduction of dentin formation does not depend on apoptosis of dental epithelium and mesenchymal cells.

Laminin α2 did not enhance proliferation and caused no cell binding activity in the primary cultured dental mesenchymal cells; however, it did regulate the expression of dentin matrix. In contrast, type I collagen and fibronectin showed cell binding activity and enhanced the proliferation of dental mesenchymal cells. Matrix expression in primary cultured tooth germ cells was affected by cell proliferation and cell binding (26). In fact, type I collagen enhanced proliferation of both dental epithelial and mesenchymal cells and showed cell binding activity, as well as in a previous report (26). These results suggest that laminin-2 has a different function with dental mesenchymal cells, especially in contrast to odontoblasts. In addition, laminin-2 coating enhanced the expression of Dsp and Dmp, and this effect was specific to laminin-2 and corresponded to the expression of these genes in laminin α2 null mutant mice.

We also considered what kind of molecules had an interaction with laminin α2 and regulated the expression of dentin matrix proteins during dentin formation. Laminin interacts

with several types of extracellular matrix and cell receptors. For example, laminin 5 ($\alpha3\beta3\gamma2$) differentially regulates the anchorage and motility of epithelial cells through integrin $\alpha_6\beta_4$ and $\alpha_3\beta_1$, respectively (47). Furthermore, targeted disruption of the *LAMA3* gene, which encodes the α3 subunit of laminin-5, caused an abnormality similar to human junctional epidermolysis bullosa and disturbed ameloblast differentiation (16). These results suggest that laminin is important for tooth formation. The laminin-type G (LG) domain modules consist of ~190 residues at the C-terminal of the laminin α1 to α5 chains (4); however, the function of the G domain of the laminin α2 chain, which is shared by laminin-2 and -4, has not been extensively studied. It has also been demonstrated that the absence of α2 chains in two mutant mouse strains caused severe muscular dystrophy, presumably because of a strong muscular matrix interaction (11, 12). Other indications for the potential functions of α2LG modules have come from previous studies of laminin-2 and -4, which demonstrated cell adhesion through β_1 integrin and heparin binding (48), and a distinct interaction with α-dystroglycan (49, 50). Moreover, the β_1 integrin is expressed in dental mesenchymal cells and differentiated odontoblasts and may interact with laminin α2 during dentin formation. In addition, the heparan sulfate proteoglycan perlecan also binds to the LG module of laminin α2 (51), is expressed in dental mesenchymal cells, and localized in the BM of the tooth germ (data not shown). Our preliminary experiment showed that cell binding of dental epithelium to laminin-2 was inhibited by the addition of EDTA and RGD peptide. Furthermore, the enhancement of DMP and DSPP mRNA expression in dental mesenchymal cells by laminin-2 was inhibited by the addition of heparin. These results suggest that laminin-2 interacts with integrins in dental epithelial cells and heparan sulfate proteoglycan in dental mesenchymal cells, and regulates the cell binding involved with dental epithelium and dentin matrix expression. These molecules may be candidates for the partner of laminin α2 in the tooth germ and are now under investigation in our laboratory using inhibitory antibodies to integrins and recombinant proteins for perlecan.

The present results indicate that absence of the laminin α2 chain and altered regulation of dentin matrix proteins may be causative factors that contribute to mineralization defects in tooth developments disorders.

Acknowledgment—We thank Dr. Yoshihiko Yamada for helpful discussion, critical comments, and providing the antibodies.

REFERENCES

1. Lumsden, A. G. (1988) *Development* **103,** (suppl.) 155–169
2. Ruch, J. V. (1987) *Rev. Biol. Cell.* **14,** 1–99
3. Thesleff, I., and Hurmerinta, K. (1981) *Differentiation* **18,** 75–88
4. Timpl, R. (1996) *Curr. Opin. Cell Biol.* **8,** 618–624
5. Yurchenco, P. D., and O'Rear, J. J. (1994) *Curr. Opin. Cell Biol.* **6,** 674–681
6. Patton, B. L., Miner, J. H., Chiu, A. Y., and Sanes, J. R. (1997) *J. Cell Biol.* **139,** 1507–1521
7. Tome, F. M., Evangelista, T., Leclerc, A., Sunada, Y., Manole, E., Estournet, B., Barois, A., Campbell, K. P., and Fardeau, M. (1994) *C. R. Acad. Sci. III (Paris)* **317,** 351–357
8. Shorer, Z., Philpot, J., Muntoni, F., Sewry, C., and Dubowitz, V. (1995) *J. Child Neurol.* **10,** 472–475
9. Sewry, C. A., Uziyel, Y., Torelli, S., Buchanan, S., Sorokin. L., Cohen, J., and Watt, D. J. (1998) *Neuropathol. Appl. Neurobiol.* **24,** 66–72
10. Sunada, Y., Bernier, S. M., Kozak, C. A., Yamada, Y., and Campbell, K. P. (1994) *J. Biol. Chem.* **269,** 13729–13732
11. Xu, H., Christmas, P., Wu, X. R., Wewer, U. M., and Engvall, E. (1994) *Proc. Natl. Acad. Sci. U. S. A.* **91,** 5572–5576
12. Miyagoe, Y., Hanaoka, K., Nonaka, I., Hayasaka, M., Nabeshima, Y., Arahata, K., and Takeda, S. (1997) *FEBS Lett.* **415,** 33–39
13. Miyagoe-Suzuki, Y., Nakagawa, M., and Takeda, S. (2000) *Microsc. Res. Tech.* **48,** 181–191
14. Salmivirta, K., Sorokin, L. M., and Ekblom, P. (1997) *Dev. Dyn.* **210,** 206–215
15. Salmivirta, K., and Ekblom, P. (1998) *Ann. N. Y. Acad. Sci.* **857,** 279–282
16. Ryan, M. C., Lee, K., Miyashita, Y., and Carter, W. G. (1999) *J. Cell Biol.* **145,** 1309–1323
17. Krebsbach, P. H., Lee, S. K., Matsuki, Y., Kozak, C. A., Yamada, K. M., and Yamada, Y. (1996) *J. Biol. Chem.* **271,** 4431–4435
18. Simmer, J. P., Lau, E. C., Hu, C. C., Aoba, T., Lacey, M., Nelson, D., Zeichner-David, M., Snead, M. L., Slavkin, H. C., and Fincham, A. G. (1994) *Calcif. Tissue Int.* **54,** 312–319
19. Diekwisch, T. G., Ware, J., Fincham, A. G., and Zeichner-David, M. (1997) *J. Histochem. Cytochem.* **45,** 859–866
20. Fisher, L. W., Stubbs, J. T., III, and Young, M. F. (1995) *Acta Orthop. Scand. Suppl.* **266,** 61–65
21. Fukumoto, E., Sakai, H., Fukumoto, S., Yagi, T., Takagi, O., and Kato, Y. (2003) *J. Dent. Res.* **82,** 17–22
22. Kawano, S., Morotomi, T., Toyono, T., Nakamura, N., Uchida, T., Ohishi, M., Toyoshima, K., and Harada, H. (2002) *Connect. Tissue Res.* **43,** 409–412
23. Schuler, F., and Sorokin, L. M. (1995) *J. Cell Sci.* **108,** 3795–3805
24. Lesot, H., Osman, M., and Ruch, J. V. (1981) *Dev. Biol.* **82,** 371–381
25. Thesleff, I., Barrach, H. J., Foidart, J. M., Vaheri, A., Pratt, R. M., and Martin, G. R. (1981) *Dev. Biol.* **81,** 182–192
26. Kukita, A., Harada, H., Kukita, T., Inai, T., Matsuhashi, S., and Kurisu, K. (1992) *Calcif. Tissue Int.* **51,** 393–398
27. Smith, C. E., and Chen, W. Y. (1998) *Connect. Tissue Res.* **39,** 75–87, 141–149
28. Cerny, R., Slaby, I., Hammarstrom, L., and Wurtz, T. (1996) *J. Bone Miner. Res.* **11,** 883–891
29. Fong, C. D., Hammarstrom, L., Lundmark, C., Wurtz, T., and Slaby, I. (1996) *Adv. Dent. Res.* **10,** 195–200
30. Lee, S. K., Krebsbach, P. H., Matsuki, Y., Nanci, A., Yamada, K. M., and Yamada, Y. (1996) *Int. J. Dev. Biol.* **40,** 1141–1150
31. Leach, N. J., and Winter, G. B. (1995) *Hum. Mutat.* **5,** 251–259
32. Lagerstrom, M., Dahl, N., Nakahori, Y., Nakagome, Y., Backman, B., Landegren, U., and Pettersson, U. (1991) *Genomics* **10,** 971–975
33. Collier, P. M., Sauk, J. J., Rosenbloom, S. J., Yuan, Z. A., and Gibson, C. W. (1997) *Arch. Oral Biol.* **42,** 235–242
34. Gibson, C. W., Yuan, Z. A., Hall, B., Longenecker, G., Chen, E., Thyagarajan, T., Sreenath, T., Wright, J. T., Decker, S., Piddington, R., Harrison, G., and Kulkarni, A. B. (2001) *J. Biol. Chem.* **276,** 31871–31875
35. MacDougall, M., DuPont, B. R., Simmons, D., Reus, B., Krebsbach, P., Karrman, C., Holmgren. G., Leach, R. J., and Forsman, K. (1997) *Genomics* **41,** 115–118
36. MacDougall. M., Simmons, D., Luan, X., Nydegger, J., Feng, J., and Gu, T. T. (1997) *J. Biol. Chem.* **272,** 835–842
37. Feng, J. Q., Luan, X., Wallace, J., Jing, D., Ohshima, T., Kulkarni, A. B., D'Souza, R. N., Kozak, C. A., and MacDougall, M. (1998) *J. Biol. Chem.* **273,** 9457–9464
38. D'Souza, R. N., Bronckers, A. L., Happonen, R. P., Doga, D. A., Farach-Carson, M. C., and Butler, W. T. (1992) *J. Histochem. Cytochem.* **40,** 359–366
39. Begue-Kirn, C., Krebsbach, P. H., Bartlett, J. D., and Butler, W. T. (1998) *Eur. J. Oral Sci.* **106,** 963–970
40. D'Souza, R. N., Cavender, A., Sunavala, G., Alvarez, J., Ohshima, T., Kulkarni, A. B., and MacDougall, M. (1997) *J. Bone Miner. Res.* **12,** 2040–2049
41. Xiao, S., Yu, C., Chou, X., Yuan, W., Wang, Y., Bu, L., Fu, G., Qian, M., Yang, J., Shi, Y., Hu, L., Han, B., Wang, Z., Huang, W., Liu, J., Chen, Z., Zhao, G., and Kong, X. (2001) *Nat. Genet.* **27,** 201–204
42. Zhang, X., Zhao, J., Li, C., Gao, S., Qiu, C., Liu, P., Wu, G., Qiang, B., Lo, W. H., and Shen, Y. (2001) *Nat. Genet.* **27,** 151–152
43. Sreenath, T., Thyagarajan, T., Hall, B., Longenecker, G., D'Souza, R., Hong, S., Wright, J. T., MacDougall, M., Sauk, J., and Kulkarni, A. B. (2003) *J. Biol. Chem.* **278,** 24874–24880
44. Hoshi, K., Kemmotsu, S., Takeuchi, Y., Amizuka, N., and Ozawa, H. (1999) *J. Bone Miner. Res.* **14,** 273–280
45. Boskey, A. L., Spevak, L., Doty, S. B., and Rosenberg, L. (1997) *Calcif. Tissue Int.* **61,** 298–305
46. Vachon, P. H., Loechel, F., Xu, H., Wewer, U. M., and Engvall, E. (1996) *J. Cell Biol.* **134,** 1483–1497
47. Nguyen, B. P., Gil, S. G., and Carter, W. G. (2000) *J. Biol. Chem.* **275,** 31896–31907
48. Brown, J. C., Wiedemann, H., and Timpl, R. (1994) *J. Cell Sci.* **107,** 329–338
49. Yamada, H., Shimizu, T., Tanaka, T., Campbell, K. P., and Matsumura, K. (1994) *FEBS Lett.* **352,** 49–53
50. Pall, E. A., Bolton, K. M., and Ervasti, J. M. (1996) *J. Biol. Chem.* **271,** 3817–3821
51. Talts, J. F., Andac, Z., Gohring, W., Brancaccio, A., and Timpl, R. (1999) *EMBO J.* **18,** 863–870

Atherosclerosis in perlecan heterozygous mice

Reeba K. Vikramadithyan,* Yuko Kako,* Guangping Chen,* Yunying Hu,* Eri Arikawa-Hirasawa,† Yoshihiko Yamada,† and Ira J. Goldberg[1],*

Department of Medicine,* Columbia University, New York, NY 10032; and National Institute of Dental and Craniofacial Research,† Bethesda, MD 20892-4370

Abstract **The hypothesis that lipoprotein association with perlecan is atherogenic was tested by studying atherosclerosis in mice that had a heterozygous deletion of perlecan, the primary extracellular heparan sulfate proteoglycan in arteries. We first studied the expression of perlecan in mouse lesions and noted that this proteoglycan in aorta was found in the subendothelial matrix. Perlecan was also a major component of the lesional extracellular matrix. Mice with a heterozygous deletion had a reduction in arterial wall perlecan expression. Atherosclerosis in these mice was studied after crossing the defect into the apolipoprotein E (apoE) and LDL receptor knockout backgrounds. At 12 weeks, chow-fed apoE null mice with a heterozygous deletion had less atherosclerosis. However, at 24 weeks and in the LDL receptor heterozygous background, the presence of a perlecan knockout allele did not significantly alter lesion size. Thus, it appears that loss of perlecan leads to less atherosclerosis in early lesions. Although this might be attributable to a decrease in lipoprotein retention, it should be noted that perlecan might mediate multiple other processes that could, in sum, accelerate atherosclerosis.**—Vikramadithyan, R. K., Y. Kako, G. Chen, Y. Hu, E. Arikawa-Hirasawa, Y. Yamada, and I. J. Goldberg. **Atherosclerosis in perlecan heterozygous mice.** *J. Lipid Res.* **2004. 45: 1806–1812.**

Supplementary key words heparan • low density lipoprotein receptor • apolipoprotein E • proteoglycans • lipoproteins

Much of atherosclerosis research in the 20th century focused on the cholesterol hypothesis. The evidence that plasma cholesterol-containing lipoproteins cause atherosclerosis is indisputable. However, as was nicely summarized nearly 50 years ago (1), how these lipid-containing particles accumulate within the artery and then produce inflammatory reactions is still unclear. A refinement to the "infiltrative theory" has been an attempt to define the biochemical interactions that lead to this process. Because the lipoproteins are initially found in the extracellular space, they are thought to bind to protein or carbohydrate components of the extracellular matrix. Among the molecules that have been most studied in this respect are proteoglycans (2).

Within the artery are a number of classes of proteoglycans, complex proteins that contain highly negatively charged carbohydrates. There are several observations that support the proteoglycan-lipoprotein association hypothesis. *1*) Dermatan/chondroitin sulfate proteoglycans are found in greater amounts in lesions (3, 4), and some classes of these proteins are found in regions that also contain apolipoprotein B (apoB) (5), the major protein component of LDL and remnant lipoproteins. *2*) Complexes of proteoglycans and LDL have been isolated from arteries (6). *3*) Prolonged incubations of proteoglycans and LDL will, in vitro, produce aggregates (7).

Of all the proteoglycans, the most heavily charged and most avid LDL binding are the heparan sulfate proteoglycans (8). Heparin, a highly charged carbohydrate of this class, has been studied because it interacts with apoB-containing lipoproteins (9, 10). This reaction, however, is most evident in low ionic strength solutions; in several reports, the proteoglycan-LDL complexes are dissociated by physiologic saline (9). Moreover, increasing LDL charge (e.g., via oxidation) decreases the proteoglycan-lipoprotein interaction (11).

One way to study the role of proteoglycans in atherosclerosis is to use genetically manipulated mice that have an alteration in proteoglycan production. Perlecan is a 450 kDa core protein containing three heparan sulfate chains of 70 kDa attached in domain I and an additional chain associated with domain V. Perlecan is the major heparan sulfate proteoglycan in the subendothelial matrix (12). This protein has a variety of actions and is essential for normal bone formation and neurological development; a homozygous deletion of perlecan in mice is lethal as a result of bone and neurological malformations (13). Within the vasculature, perlecan helps to stabilize the endothelial barrier and decrease the proliferation of smooth muscle cells (14); these are potentially antiatherogenic actions of perlecan. We first studied perlecan expression

Manuscript received 21 January 2004, in revised form 2 June 2004, and in re-revised form 8 July 2004.

Published, JLR Papers in Press, July 16, 2004.
DOI 10.1194/jlr.M400019-JLR200

[1]To whom correspondence should be addressed.
e-mail: ijg3@columbia.edu

in normal and atherosclerotic mouse arteries and then tested whether a partial loss of perlecan alters atherosclerosis in the mouse.

METHODS

Mouse housing and diets

Mice were maintained in a temperature-controlled (25°C) facility with a 12 h light/dark cycle and given free access to food and water, except when fasting blood specimens were obtained. Mice were fed either laboratory rodent chow (PMI Nutrition International, Inc.) or a Paigen diet (C13002; Research Diets, Inc.). Rodent chow contained 4.5% (w/w) fat; the Paigen diet contained 15% (w/w) fat, 1.25% (w/w) cholesterol, and 0.5% cholic acid.

Genetically altered mice

Heterozygous perlecan-deficient mice (13) were backcrossed to C57BL/6 mice for seven generations. These animals were crossed onto apolipoprotein E null (apoE0) mice or LDL receptor knockout mice in the same background that were purchased from Jackson Laboratory (Bar Harbor, ME).

Immunohistochemical staining for aortic perlecan

Aortas from male apoE0 mice fed a chow diet at different time points were embedded in OCT and snap frozen on dry ice. Ten micrometer frozen sections were fixed in cold acetone, and endogenous peroxidase was quenched with 3% H_2O_2/methanol. The sections were then stained with 1:100 rat monoclonal antibody against perlecan (Neo Marks, Inc.) at 37°C for 1 h, then at 4°C overnight. The antibody was detected with the standard Avidin Biotin Complex method (Vector Laboratories, Inc.) and 3-amino-9-ethyl carbazole (Zymed Laboratories) as the substrate. Positive staining is shown as red deposits. For a negative control, slides were incubated with nonimmune rat IgG (Sigma) in place of the first antibody.

Quantitative real-time PCR for the aortic perlecan gene

Total RNA was isolated from aortas of heterozygous LDL receptor-deficient mice and heterozygous perlecan mice in the heterozygous LDL receptor-deficient background using the RNeasy mini kit (Qiagen). The mRNA levels for perlecan were determined by SYBR green (Applied Biosystems) real-time PCR using 10–100 ng of total RNA. Primer sequences were selected from domain I, the potential heparan sulfate attachment domain (PubMed sequence NM008305; 201–408). The primer sequences are as follows: Prl-RT (forward), 5′-TACGCGGTCCATTGAG-3′; Prl-RT (reverse), 5′-AGATCCGTCCGCATTC-3′. The real-time PCR standard curve was constructed by using serial dilutions of mouse total RNA isolated from aortas. Data were normalized to mouse β-actin.

Blood sampling

Fasting blood samples were obtained from mice after removal of food for 6 h in the morning. The animals were anesthetized with methoxyflurane and bled by retro-orbital phlebotomy into tubes containing anticoagulant (5 mM EDTA) using heparinized capillary tubes. Cholesterol and triglyceride were measured using kits from Sigma. Lipoproteins—VLDL ($d < 1.006$ g/ml), intermediate density lipoprotein/LDL ($d = 1.006$–1.063 g/ml), and HDL ($d = 1.063$–1.21 g/ml)—were separated by sequential density ultracentrifugation of plasma in a TLA 100 rotor (Beckman Instruments) (15).

Quantitative atherosclerosis analysis

Mice were killed and atherosclerosis assays were performed on the aortic roots as described previously (15, 16). Hearts were perfused with PBS, fixed in 10% phosphate-buffered formalin, embedded in OCT compound, and sectioned with a cryostat at 10 μm thickness. Slides containing the aortic tissue were stained with Oil Red O and hematoxylin and counterstained with light green. Lesions of the proximal aorta were measured in 80 μm intervals. The mean lesion area of six sections was calculated and shown as lesion area (μm^2). The atherosclerotic lesions were assessed by en face assays (17).

Statistical analysis

Comparisons between two genotypes were performed using a two-tailed Student's *t*-test.

RESULTS

Perlecan expression in blood vessels

The expression of perlecan within the aorta of apoE mice fed a chow diet differed markedly as a function of

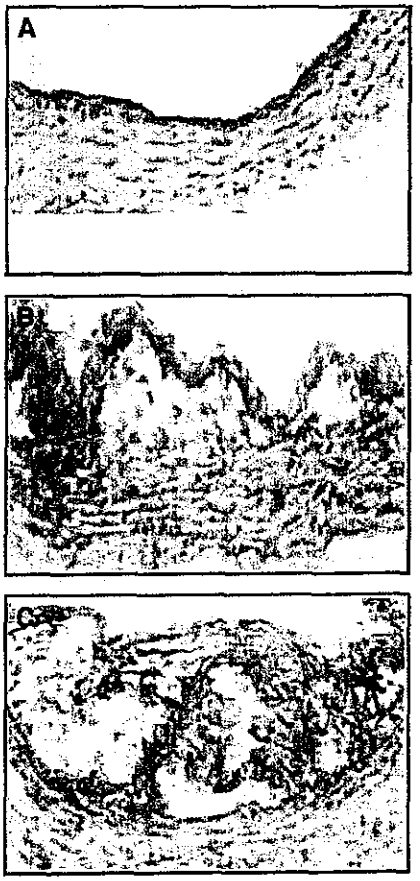

Fig. 1. Perlecan expression in lesions of atherosclerosis varies with lesion severity. A: In normal aorta, perlecan was distributed in the subendothelial regions. B,C: Perlecan expression increased markedly in advanced lesions, in the fibrous cap as well as in the plaque core.

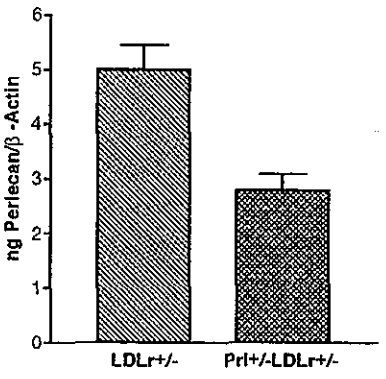

Fig. 2. Perlecan expression in aortas by quantitative real-time PCR. Aortas from heterozygous LDL receptor (LDLr)-deficient mice and heterozygous perlecan (Prl) mice in the heterozygous LDL receptor-deficient background were used for real-time PCR. Aortas from three mice from each group were pooled for RNA per set. The data shown are averages of two sets. Values are expressed as mean ± SEM.

disease within the vessel. In normal, nondiseased aortas, perlecan staining was primarily localized to the subendothelial regions (**Fig. 1A**). In more advanced lesions, additional staining was found within the fibrous cap that would be expected to have proliferated smooth muscle cells (Fig. 1B). Most remarkably, in advanced lesions with lipid-filled cores, intense staining was within the lipid core (Fig. 1C). Thus, perlecan is a major matrix protein within the lesions.

Quantitative real-time PCR for the aortic perlecan gene

To determine whether heterozygous perlecan knockout mice have an alteration of perlecan expression, the aortic content of perlecan mRNA was compared with that of control mice. A shown in **Fig. 2**, deletion of one allele reduced perlecan expression.

Lipids in perlecan heterozygous knockout mice

Because lipoprotein uptake by the liver is thought to be mediated, in part, by "capture" by proteoglycans, we assessed whether the loss of perlecan would alter plasma lipoproteins. **Table 1** shows plasma and lipoprotein lipids of wild-type and perlecan heterozygous mice eating chow and a Paigen diet. Both strains of mice had identical levels of plasma cholesterol and triglyceride, VLDL, LDL, and HDL. This was confirmed by FPLC analysis (data not shown). When these mice were placed on a Paigen diet, both the controls and perlecan heterozygous mice had a similar increase in plasma apoB-containing lipoproteins. However, loss of perlecan did not affect lipids.

Lipoprotein uptake via receptors might have obscured any uptake as a result of liver or peripheral tissue heparan sulfate proteoglycan-mediated processes. Therefore, we next examined lipids and lipoproteins in apoE0 and apoE0/perlecan heterozygous mice. As expected, compared with wild-type mice, apoE deficiency led to marked increases of cholesterol and triglyceride at 12 weeks of age (**Table 2**). However, perlecan deficiency did not significantly alter plasma cholesterol, which was 420 ± 105 mg/dl for apoE0 mice and 359 ± 114 mg/dl for apoE0/perlecan heterozygous mice. A second group of mice was maintained on this diet for 24 weeks (Table 2). Again, the lipids and lipoproteins were not different. Therefore, perlecan deficiency did not alter either plasma or lipoprotein lipids in the apoE0 background.

Perlecan-deficient mice were then crossed with LDL receptor knockouts. Because our primary objective was to study atherosclerosis, we created a colony of heterozygous LDL receptor knockouts and fed them the Paigen diet as reported by van Haperen et al. (18). Male LDL receptor heterozygous ($LDL^{+/-}$) and perlecan-deficient $LDL^{+/-}$ mice were begun on a Paigen diet at 4 weeks of age and maintained on this diet for 16 weeks. Plasma cholesterol in these mice averaged 579 ± 33 and 595 ± 32 mg/dl in $LDL^{+/-}$ and perlecan-deficient/LDL receptor-deficient mice, respectively (**Table 3**).

Atherosclerosis in control and perlecan heterozygous apoE0 mice

In the chow-fed apoE knockout mice, both early lesions (12 weeks) and later lesions (24 weeks) were studied. In 12 week old male mice, perlecan deficiency led to a dramatic and significant reduction in lesion size, which averaged 23,961 μm^2 in controls and 7,796 μm^2 in perlecan heterozygous animals ($P = 0.02$) (**Table 4**). Lesion sizes for individual animals are shown in **Fig. 3A**, graphed on a semi-log scale. Lack of perlecan led to a >70% reduction

TABLE 1. Lipid profiles of wild-type and heterozygous perlecan-deficient mice fed chow and Paigen diets

				Cholesterol				Triglyceride	
Genotype	Diet	Age	n	Plasma	VLDL	LDL	HDL	Plasma	VLDL
		weeks		*mg/dl*				*mg/dl*	
Wild-type	Chow	15	5	83 ± 12	21 ± 13	23 ± 4	55 ± 10	50 ± 14	17 ± 8
$Prl^{+/-}$	Chow	15	5	95 ± 20	17 ± 4	27 ± 10	63 ± 24	52 ± 19	13 ± 5
Wild-type	Paigen	19	4	236 ± 36	123 ± 23	68 ± 6	48 ± 8	48 ± 2	25 ± 2
$Prl^{+/-}$	Paigen	19	5	248 ± 36	151 ± 34	59 ± 4	48 ± 7	50 ± 10	25 ± 5
Wild-type	Paigen	40	4	198 ± 27	114 ± 27	33 ± 4	41 ± 13	44 ± 9	27 ± 9
$Prl^{+/-}$	Paigen	40	5	199 ± 2	112 ± 15	34 ± 3	45 ± 9	49 ± 6	31 ± 6

Blood samples were obtained at 15 weeks of age for the chow diet-fed state and at 19 weeks and 10 months of age for the Paigen diet-fed state. Prl+/− denotes mice that have a heterozygous deletion of the perlecan gene.

TABLE 2. Lipid profiles of heterozygous perlecan-deficient mice in the apoE0 background

Genotype	Gender	n	Cholesterol				Triglyceride	
			Plasma	VLDL	LDL	HDL	Plasma	VLDL
			mg/dl				*mg/dl*	
12 weeks of age								
apoE0	Male	13	420 ± 105	311 ± 115	82 ± 23	23 ± 7	120 ± 35	88 ± 27
apoE0/Prl$^{+/-}$	Male	13	359 ± 114	257 ± 113	71 ± 19	23 ± 7	115 ± 20	89 ± 16
apoE0	Female	18	378 ± 101	264 ± 62	76 ± 29	14 ± 5	58 ± 12	38 ± 9
apoE0/Prl$^{+/-}$	Female	13	392 ± 87	288 ± 55	84 ± 22	14 ± 5	67 ± 14	44 ± 16
24 weeks of age								
apoE0	Male	10	487 ± 160	404 ± 156	79 ± 25	19 ± 7	127 ± 30	106 ± 27
apoE0/Prl$^{+/-}$	Male	19	418 ± 162	320 ± 158	65 ± 21	15 ± 7	116 ± 52	92 ± 49
apoE0	Female	10	401 ± 109	302 ± 96	73 ± 19	8 ± 6	49 ± 12	29 ± 11
apoE0/Prl$^{+/-}$	Female	17	405 ± 95	308 ± 82	65 ± 2	6 ± 4	50 ± 12	32 ± 10

Lipoprotein profiles were assessed by ultracentrifugation. apoE0, apolipoprotein E knockout mice; apoE0/Prl$^{+/-}$, heterozygous perlecan-deficient mice in the apoE knockout background.

in lesion size. This amount of atherosclerosis was too small to allow for en face quantification. Lesion size in female mice is also shown in Table 4 and Fig. 3A. Although a trend toward reduced lesions was noted in the perlecan heterozygous females, this was not significant.

After 24 weeks, male perlecan heterozygous mice still had, on average, less atherosclerosis, 121,961 μm^2 in controls and 89,167 μm^2 in perlecan heterozygous animals, but this difference was not significant (Fig. 3B). Female mice had larger lesions, but there was no difference with the presence of a perlecan knockout allele. En face assays also showed no difference in lesion area with perlecan deficiency, 2.8 ± 2% in apoE0 mice and 1.9 ± 1.2% in apoE0/perlecan heterozygous mice (average ± SD, $P = 0.2$).

Atherosclerosis in heterozygous LDL receptor-deficient mice

It has been hypothesized that the interaction of lipoproteins with proteoglycans might differ in mice that express apoE (19), a stronger proteoglycan binding protein than apoB. For this reason, we assessed whether a similar degree of atherosclerosis in heterozygous LDL receptor knockout mice would still show the effects of perlecan deficiency on atherosclerosis. For this reason, male mice were studied at 20 weeks. As shown in **Fig. 4**, perlecan deficiency did not alter atherosclerosis in this model. The average lesion areas in heterozygous LDL receptor-deficient and heterozygous perlecan-deficient mice in the LDL receptor heterozygous background are shown in **Table 5**.

DISCUSSION

Crossing perlecan heterozygous mice into an atherosclerotic background tested the hypothetical role for heparan sulfate proteoglycans in atherogenesis. Our data show the following. *1*) Although perlecan is primarily found in the subendothelial matrix in normal vessels, it is found in core regions of advanced atherosclerotic lesions. *2*) Despite a possible role of perlecan in the removal of lipoproteins from the circulation, a heterozygous deletion of perlecan did not alter plasma lipoprotein profiles. *3*) Young perlecan heterozygous knockout/apoE0 male mice had reduced atherosclerosis. A similar trend occurred in females. However, older mice and heterozygous LDL receptor-deficient mice had no difference in lesion size.

Endothelial cells produce a number of heparan sulfate proteoglycans when assessed in cultured cells. These include syndecans, which are a component of the cell membrane (20). Perlecan is the major heparan sulfate proteoglycan within the subendothelial matrix; some perlecan is also found associated with the apical side of the cells. Cultured smooth muscle cells express and secrete perlecan (14). Our immunohistological data suggest that both cells express perlecan in vivo, but at different times and under different stimuli. In normal vessels, perlecan was prominently found within the subendothelial matrix. However, with the development of lesions, perlecan staining was decreased in the subendothelial region. In humans, this may result in the decrease in arterial heparan sulfate proteoglycans reported with atherosclerosis (21).

TABLE 3. Lipid profiles of heterozygous perlecan-deficient mice in the LDL receptor heterozygous background on the Paigen diet for 16 weeks

Genotype	n	Cholesterol				Triglyceride	
		Plasma	VLDL	LDL	HDL	Plasma	VLDL
		mg/dl				*mg/dl*	
LDLr$^{+/-}$	13	579 ± 33	353 ± 44	219 ± 31	59 ± 5	55 ± 3	31 ± 2
LDLr$^{+/-}$/Prl$^{+/-}$	13	551 ± 30	307 ± 24	167 ± 11	62 ± 4	48 ± 3	23 ± 2

Lipoprotein profiles were assessed by ultracentrifugation. LDLr$^{+/-}$, heterozygous LDL receptor knockout mice; LDLr$^{+/-}$/Prl$^{+/-}$, heterozygous perlecan-deficient mice in the heterozygous LDL receptor background.

TABLE 4. Atherosclerotic lesions of heterozygous perlecan-deficient mice in the apoE0 background

Genotype	Gender	12 Weeks of Age n	12 Weeks of Age Lesion Size (μm^2)	24 Weeks of Age n	24 Weeks of Age Lesion Size (μm^2)
apoE0	Male	13	23,961 ± 26,075	11	121,961 ± 71,643
apoE0/Prl$^{+/-}$	Male	11	7,796 ± 7,949[a]	19	89,167 ± 49,978
apoE0	Female	13	28,940 ± 45,369	10	205,004 ± 107,623
apoE0/Prl$^{+/-}$	Female	14	19,789 ± 22,302	17	180,142 ± 63,035

[a] $P < 0.05$ compared with apoE0 mice.

The reasons for this decrease might be altered perlecan expression or an increase in its degradation. The latter might result from the actions of heparanase, which is secreted by endothelial cells in response to atherogenic stimuli (22).

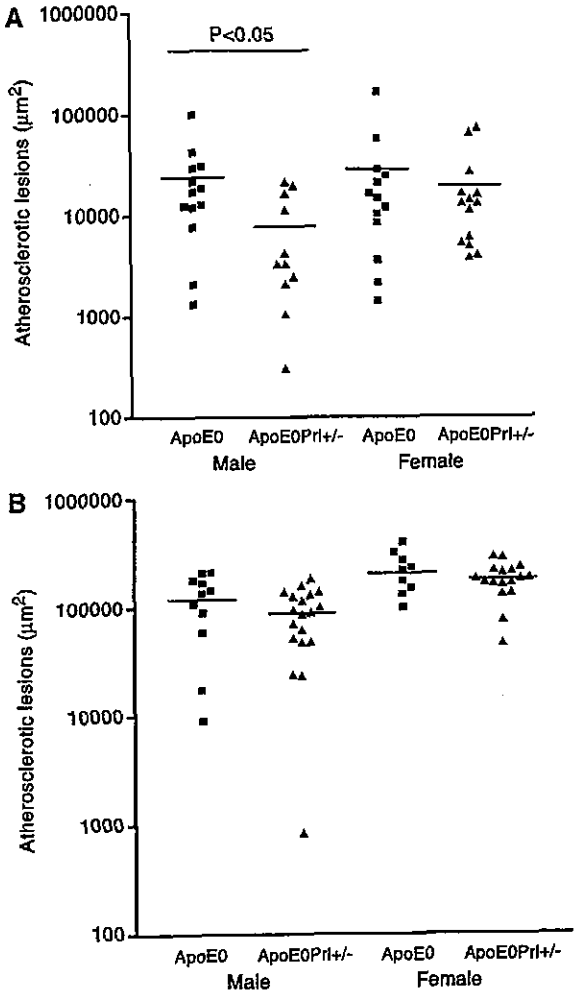

Fig. 3. Effects of heterozygous perlecan deficiency on atherosclerotic lesions. Heterozygous perlecan deficiency was crossed into the apoE knockout background. Male and female chow-fed mice were assessed for lipids and atherosclerosis after 12 weeks (A) and 24 weeks (B). The data obtained from sections of the aortic root are shown on a log scale. $P < 0.05$.

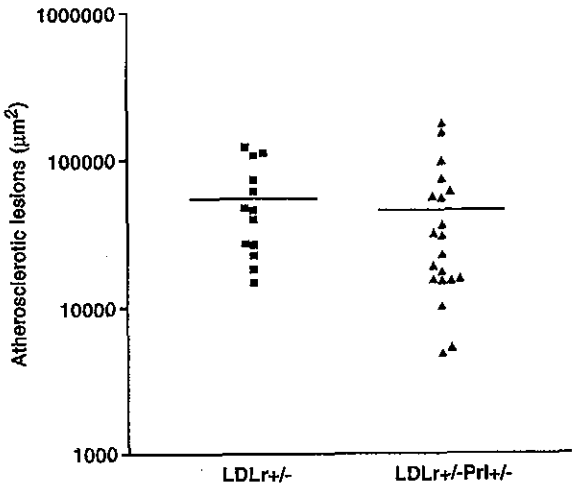

Fig. 4. Atherosclerosis in LDL receptor (LDLr) heterozygous knockout mice. Perlecan (Prl) heterozygous knockout mice were bred with LDL receptor knockout mice. The offspring, all with a heterozygous deficiency of LDL receptor, were fed a high-fat and cholesterol/cholic acid-containing diet (Paigen) for 16 weeks, and atherosclerotic lesion size at the aortic root was quantified.

Kunjathoor et al. (23) have demonstrated that the major proteoglycans detected in murine atherosclerosis are perlecan and biglycan. Perlecan was present extensively in the lesions of apoE-deficient and LDL receptor-deficient mice. Perlecan was also detected in intermediate and advanced lesions of hypercholesterolemic nonhuman primates and in cultures of medial smooth muscle cells from human atherosclerotic tissue. Our data comparing early and advanced lesions confirm their observations. Like others, we also found perlecan staining surrounding the lipid core (24). Moreover, we found remarkable amounts of perlecan in very advanced lesions containing necrotic lipid cores. Because these regions are distant from endothelial cells, we speculate that either smooth muscle cells or macrophages are the source of this perlecan. Because macrophages do not appear to express perlecan in great quantities (25), either smooth muscle cells or some other cells are the likely origin of most perlecan in mouse atherosclerotic lesions.

We had anticipated that perlecan deficiency would result in a defect in lipoprotein removal from the bloodstream, similar to that found in some diabetic models (26). However neither fasting nor postprandial lipemia differed between control and perlecan heterozygous mice.

TABLE 5. Atherosclerotic lesions of heterozygous perlecan-deficient mice in the LDL receptor heterozygous background

Genotype	Gender	20 Weeks of Age n	20 Weeks of Age Lesion Size (μm^2)
LDLr$^{+/-}$	Male	13	55,653 ± 10,505
LDLr$^{+/-}$/Prl$^{+/-}$	Male	20	45,361 ± 10,622

Mice were maintained on the Paigen diet for 16 weeks.

In fact, the rationale for the use of apoE0 mice was, in part, to allow us to assess the effect of perlecan deficiency on the removal of remnant lipoproteins. We hypothesized that the apoB-48-containing lipoproteins in these mice were unable to interact with either the LDL receptor or the LDL receptor-related protein and relied on heparan sulfate proteoglycan binding for removal. However, partial loss of perlecan was not physiologically significant. Perhaps the apoE-deficient lipoproteins were unable to bind to heparan sulfate proteoglycans, and therefore, perlecan deficiency had no effect.

To test some of these hypotheses, we performed a study in heterozygous LDL receptor knockout mice fed an atherogenic diet. These mice have sufficient hypercholesterolemia to develop atherosclerotic lesions, as noted by others (18); however, perlecan deficiency did not alter the lipoprotein profiles. Using heterozygous LDL receptor knockout mice, we attempted to create lesions that were similar in size to those of the 12 week old male apoE0 mice. Although the lesions were somewhat larger, perlecan deficiency did not alter the lesion size. Perhaps these lesions in the cholic acid-fed mice were more inflammatory and, hence, less affected by a gene deletion that would alter lipoprotein retention. Alternatively, the lesions studied might have been too advanced to find differences. Finally, the pathogenesis of lesions might differ in these two models as a result of the presence of apoE.

Although perlecan was a likely candidate to have affected atherosclerosis progression, the heterozygous mutation could have been expected to increase or decrease lesions. A central role for lipoprotein accumulation attributable to its binding to matrix molecules within the arterial walls was proposed almost 50 years ago by Page (1). The "infiltrative" theory of atherosclerosis suggested that plasma cholesterol-containing lipoproteins accumulate in vessels either because they are present in greater concentrations or that matrix is altered to increase the propensity for the lipoproteins to be retained within the artery. A refinement of this theory termed the "response to retention" suggested that proteoglycans are the matrix component that "traps" atherogenic lipoproteins (27). However, the biochemical evidence supporting an important role for lipoprotein-proteoglycan complexes has been questioned (28). Non-apoE-containing lipoproteins have relatively weak affinity for proteoglycans in physiological ionic conditions. This has led us (28, 29) and others (30) to suggest that lipoprotein-proteoglycan interaction requires an intermediary molecule such as lipoprotein lipase. The other lipoprotein-associating molecule that would be expected to increase lipoprotein-proteoglycan interaction, apoE, is antiatherosclerotic.

Our studies show that perlecan deficiency leads to less atherosclerosis. This was found in early, but not late, lesions of apoE0 mice. Most notable is the comparison of our data with those of Skalen et al. (19), who studied atherosclerosis in mice with an apoB mutation that decreases proteoglycan affinity. Like these authors, we found that later lesions were no longer significantly different from those of controls. In addition, like Skalen et al. (19), we failed to find a major difference in atherosclerosis when perlecan deficiency was assessed in the heterozygous LDL-deficient background. These authors postulated that apoE-containing LDL, found in mice but not in humans, has greater affinity for proteoglycans. Hence, the effects of alterations in apoB structure, and perhaps the amount of vessel wall perlecan, might be less evident in LDL receptor knockout mice.

We conclude that perlecan is a major component of advanced atherosclerotic lesions in the mouse. A heterozygous deficiency of perlecan led to reduced atherosclerosis in apoE0 mice. This effect was found in young males without advanced lesions. Although it is possible that perlecan deficiency alone reduced atherosclerosis as a result of reduced lipoprotein retention, the complexity of the process and the multiple biological actions of perlecan do not allow one to make that conclusion with certainty.

This research was funded by Grants HL-62301 and HL-56984 (SCOR) from the National Heart, Blood, and Lung Institute.

REFERENCES

1. Page, I. H. 1954. Atherosclerosis: an introduction. *Circulation.* **10:** 1–27.
2. Camejo, G., E. Hurt-Camejo, O. Wiklund, and G. Bondjers. 1998. Association of apo B lipoproteins with arterial proteoglycans: pathological significance and molecular basis. *Atherosclerosis.* **139:** 205–222.
3. Dalferes, E. R., Jr., B. Radhakrishnamurthy, H. A. Ruiz, and G. S. Berenson. 1987. Composition of proteoglycans from human atherosclerotic lesions. *Exp. Mol. Pathol.* **47:** 363–376.
4. Ehrlich, K. C., B. Radhakrishnamurthy, and G. S. Berenson. 1975. Isolation of a chondroitin sulfate–dermatan sulfate proteoglycan from bovine aorta. *Arch. Biochem. Biophys.* **171:** 361–369.
5. Radhakrishnamurthy, B., R. E. Tracy, E. R. Dalferes, Jr., and G. S. Berenson. 1998. Proteoglycans in human coronary arteriosclerotic lesions. *Exp. Mol. Pathol.* **65:** 1–8.
6. Camejo, G., F. Lalaguna, F. Lopez, and R. Starosta. 1980. Characterization and properties of a lipoprotein-complexing proteoglycan from human aorta. *Atherosclerosis.* **35:** 307–320.
7. Srinivasan, S. R., P. Vijayagopal, K. Eberle, B. Radhakrishnamurthy, and G. S. Berenson. 1989. Low-density lipoprotein binding affinity of arterial wall proteoglycans: characteristics of a chondroitin sulfate proteoglycan subfraction. *Biochim. Biophys. Acta.* **1006:** 159–166.
8. Iverius, P. H. 1972. The interaction between human plasma lipoproteins and connective tissue glycosaminoglycans. *J. Biol. Chem.* **247:** 2607–2613.
9. Camejo, G., S. O. Olofsson, F. Lopez, P. Carlsson, and G. Bondjers. 1988. Identification of Apo B-100 segments mediating the interaction of low density lipoproteins with arterial proteoglycans. *Arteriosclerosis.* **8:** 368–377.
10. Weisgraber, K. H., and S. C. Rall, Jr. 1987. Human apolipoprotein B-100 heparin-binding sites. *J. Biol. Chem.* **262:** 11097–11103.
11. Hurt-Camejo, E., G. Camejo, B. Rosengren, F. Lopez, C. Ahlstrom, G. Fager, and G. Bondjers. 1992. Effect of arterial proteoglycans and glycosaminoglycans on low density lipoprotein oxidation and its uptake by human macrophages and arterial smooth muscle cells. *Arterioscler. Thromb.* **12:** 569–583.
12. Pillarisetti, S. 2000. Lipoprotein modulation of subendothelial heparan sulfate proteoglycans (perlecan) and atherogenicity. *Trends Cardiovasc. Med.* **10:** 60–65.
13. Arikawa-Hirasawa, E., H. Watanabe, H. Takami, J. R. Hassell, and Y. Yamada. 1999. Perlecan is essential for cartilage and cephalic development. *Nat. Genet.* **23:** 354–358.
14. Paka, L., I. J. Goldberg, J. C. Obunike, S. Y. Choi, U. Saxena, I. D. Goldberg, and S. Pillarisetti. 1999. Perlecan mediates the antipro-

liferative effect of apolipoprotein E on smooth muscle cells. An underlying mechanism for the modulation of smooth muscle cell growth? *J. Biol. Chem.* **274:** 36403–36408.
15. Kako, Y., L. S. Huang, J. Yang, T. Katopodis, R. Ramakrishnan, and I. J. Goldberg. 1999. Streptozotocin-induced diabetes in human apolipoprotein B transgenic mice. Effects on lipoproteins and atherosclerosis. *J. Lipid Res.* **40:** 2185–2194.
16. Yagyu, H., E. P. Lutz, Y. Kako, S. Marks, Y. Hu, S. Y. Choi, A. Bensadoun, and I. J. Goldberg. 2002. Very low density lipoprotein (VLDL) receptor-deficient mice have reduced lipoprotein lipase activity. Possible causes of hypertriglyceridemia and reduced body mass with VLDL receptor deficiency. *J. Biol. Chem.* **277:** 10037–10043.
17. Tangirala, R. K., E. M. Rubin, and W. Palinski. 1995. Quantitation of atherosclerosis in murine models: correlation between lesions in the aortic origin and in the entire aorta, and differences in the extent of lesions between sexes in LDL receptor-deficient and apolipoprotein E-deficient mice. *J. Lipid Res.* **36:** 2320–2328.
18. van Haperen, R., A. van Tol, T. van Gent, L. Scheek, P. Visser, A. van der Kamp, F. Grosveld, and R. de Crom. 2002. Increased risk of atherosclerosis by elevated plasma levels of phospholipid transfer protein. *J. Biol. Chem.* **277:** 48938–48943.
19. Skalen, K., M. Gustafsson, E. K. Rydberg, L. M. Hulten, O. Wiklund, T. L. Innerarity, and J. Boren. 2002. Subendothelial retention of atherogenic lipoproteins in early atherosclerosis. *Nature.* **417:** 750–754.
20. Rosenberg, R. D., N. W. Shworak, J. Liu, J. J. Schwartz, and L. Zhang. 1997. Heparan sulfate proteoglycans of the cardiovascular system. Specific structures emerge but how is synthesis regulated? *J. Clin. Invest.* **100 (Suppl.):** 67–75.
21. Stevens, R. L., M. Colombo, J. J. Gonzales, W. Hollander, and K. Schmid. 1976. The glycosaminoglycans of the human artery and their changes in atherosclerosis. *J. Clin. Invest.* **58:** 470–481.
22. Sivaram, P., J. C. Obunike, and I. J. Goldberg. 1995. Lysolecithin-induced alteration of subendothelial heparan sulfate proteoglycans increases monocyte binding to matrix. *J. Biol. Chem.* **270:** 29760–29765.
23. Kunjathoor, V. V., D. S. Chiu, K. D. O'Brien, and R. C. LeBoeuf. 2002. Accumulation of biglycan and perlecan, but not versican, in lesions of murine models of atherosclerosis. *Arterioscler. Thromb. Vasc. Biol.* **22:** 462–468.
24. Evanko, S. P., E. W. Raines, R. Ross, L. I. Gold, and T. N. Wight. 1998. Proteoglycan distribution in lesions of atherosclerosis depends on lesion severity, structural characteristics, and the proximity of platelet-derived growth factor and transforming growth factor-beta. *Am. J. Pathol.* **152:** 533–546.
25. Chang, M. Y., K. L. Olin, C. Tsoi, T. N. Wight, and A. Chait. 1998. Human monocyte-derived macrophages secrete two forms of proteoglycan-macrophage colony-stimulating factor that differ in their ability to bind low density lipoproteins. *J. Biol. Chem.* **273:** 15985–15992.
26. Ebara, T., K. Conde, Y. Kako, Y. Liu, Y. Xu, R. Ramakrishnan, I. J. Goldberg, and N. S. Shachter. 2000. Delayed catabolism of apoB-48 lipoproteins due to decreased heparan sulfate proteoglycan production in diabetic mice. *J. Clin. Invest.* **105:** 1807–1818.
27. Williams, K. J., and I. Tabas. 1995. The response-to-retention hypothesis of early atherogenesis. *Arterioscler. Thromb. Vasc. Biol.* **15:** 551–561.
28. Goldberg, I. J., W. D. Wagner, L. Pang, L. Paka, L. K. Curtiss, J. A. DeLozier, G. S. Shelness, C. S. Young, and S. Pillarisetti. 1998. The NH2-terminal region of apolipoprotein B is sufficient for lipoprotein association with glycosaminoglycans. *J. Biol. Chem.* **273:** 35355–35361.
29. Saxena, U., N. M. Kulkarni, E. Ferguson, and R. S. Newton. 1992. Lipoprotein lipase-mediated lipolysis of very low density lipoproteins increases monocyte adhesion to aortic endothelial cells. *Biochem. Biophys. Res. Commun.* **189:** 1653–1658.
30. Babaev, V. R., S. Fazio, L. A. Gleaves, K. J. Carter, C. F. Semenkovich, and M. F. Linton. 1999. Macrophage lipoprotein lipase promotes foam cell formation and atherosclerosis in vivo. *J. Clin. Invest.* **103:** 1697–1705.

パールカンの多様な機能の解明をめざして

平澤(有川)　恵理　順天堂大学老人性疾患病態治療研究センター

はじめに

パールカンはすべての基底膜に存在するほか、軟骨などに存在するヘパラン硫酸プロテオグリカンである。５つの機能ドメインからなるコアタンパク質は400kDaに及び、N末とC末端にヘパラン硫酸鎖の結合部位が存在する。パールカンは成長因子シグナルを修飾し、細胞の増殖、分化を制御するなどの種々の生物学的活性を持つ[1-4]。ヘパラン硫酸プロテオグリカンには膜貫通型のシンデカンファミリー、GPI（Glycosyl Phosphatidyl Inositol）アンカー型のグリピカンファミリーもあるが、細胞外マトリックス型のパールカンは細胞表面や、細胞外マトリックス中への局在様式から、種種の成長因子、マトリックス分子、接着分子等の空間的配置や機能を巧妙に調整する働きが推察される。さらにコアタンパク質の５つのドメインはドメイン特異的な結合能を持つことからヘパラン硫酸鎖と補助的に働き特異的なシグナル伝達に寄与すると考えられる（図１）。実際、遺伝子改変マウスの解析や、ヒト遺伝性疾患の同定によりパールカンの発生や疾患における重要性が近年明らかになってきた。

遺伝子改変マウスの作成とパールカンの機能解明

パールカンの機能に関しては、10年以上前より他種類の細胞系譜を用いた *in vitro* の実験系において、非常に多くの解析がなされ多様な機能が報告されてきた。我々はパールカンの欠損

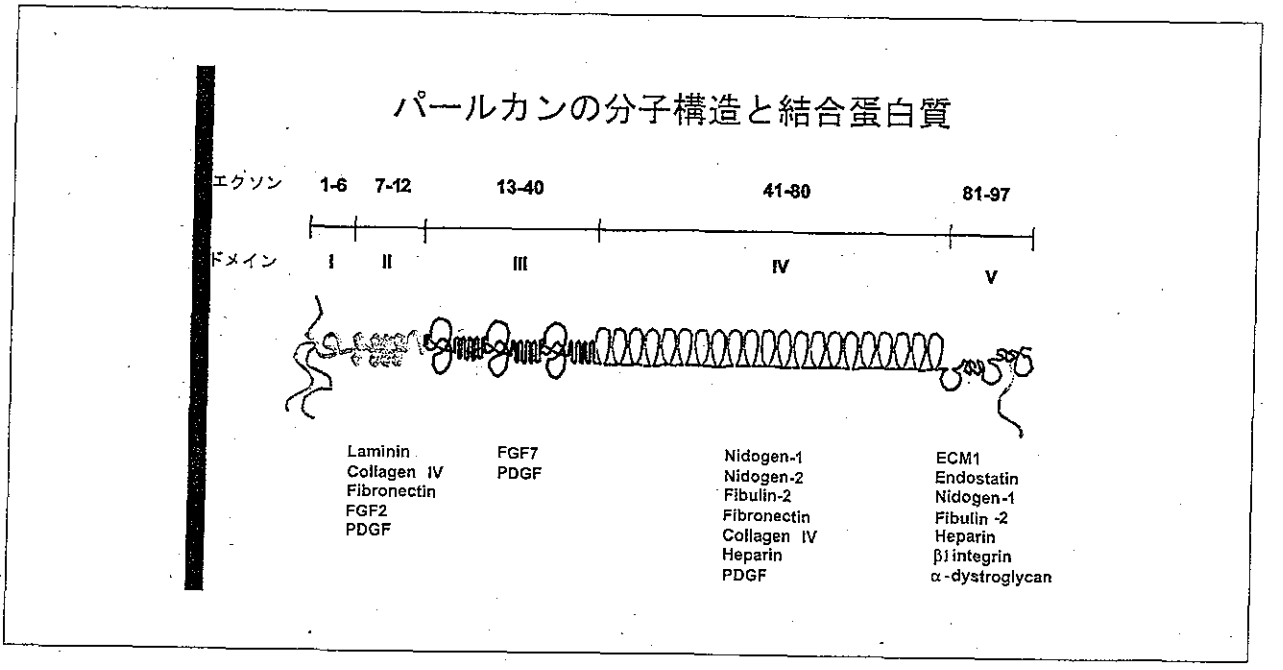

図１

が発生にどのような障害をもたらすか、また、どのような疾患に結びつくのかを調べるためには、*in vivo*での解析が必須と考えパールカン遺伝子のノックアウトマウスを作成した。パールカンは基底膜の重要な構成成分であり、さらに着床時に一過性の発現増加をみるなど初期発生における重要性も示唆されており、着床時あるいはその直後での早期胎生期致死が予測された。ところが意外なことに一部のマウスは出生まで至り、ほとんどの臓器の正常発生が確認された。一部は胎生10.5日頃に死亡するが、残りはさらに生存し胎生14.5日頃から徐々に軟骨形成異常を発症し、出生頃には明らかな四肢短縮を呈し呼吸障害を伴って死亡することが解った[5]（図2）。四肢短縮は内軟骨性骨化の障害によるが、膜性骨化は逆に亢進し、四肢の長管骨は横径が増し、太く短く発達する。脊椎の椎体部分の発生も内軟骨性骨化によるので、長管骨と同様の変化をとる。Costellらの作成したノックアウトマウスも同様の表現型を呈した[6]。パールカンノックアウトマウスにおける内軟骨性骨化の障害の原因としてはパールカン欠損により軟骨分化に深く関わるシグナル機構が変化した可能性と、軟骨マトリックス中のパールカンの欠損が他の軟骨マトリックス分子の沈着などに直接影響を与え、これを脆弱化した可能性が考えられるが、おそらくその両方の影響があると思われる。成長板での軟骨最終分化におけるシグナル機構において重要な分子としてFGF受容体3c(FGFR3c)やインディアンヘッジホグ(Ihh)等が挙げられるが、これらはヘパラン硫酸との結合が知られるので糖鎖との関連も興味深い。

ヒト遺伝性疾患の同定-二つの予後の異なる疾患におけるパールカン遺伝子の変異

我々は、ノックアウトマウスでの解析結果をもとに、ヒトでのパールカン欠損病を探索した。その結果二つの予後の異なる疾患患者でパールカン遺伝子変異を同定した。パールカンの機能完全欠損はノックアウトマウスの症状とよく似た周産期致死性のSilverman-Handmaker 型軟骨異形成症(DDSH)を、機能部分欠損では軟骨病変とミオトニア症状を併せ持つSchwartz-Jampel 症候群(SJS)を発症することを示した[7-10]。SJSの原因遺伝子の同定はこれより早くNicoleらにより報告されたが、タンパク質レベルでの解析はされておらず、二つの疾患の予後が大きく異なる原因は不明のままであった[11]。免疫組織化学的検討や初代培養からのパールカン分泌能の検討

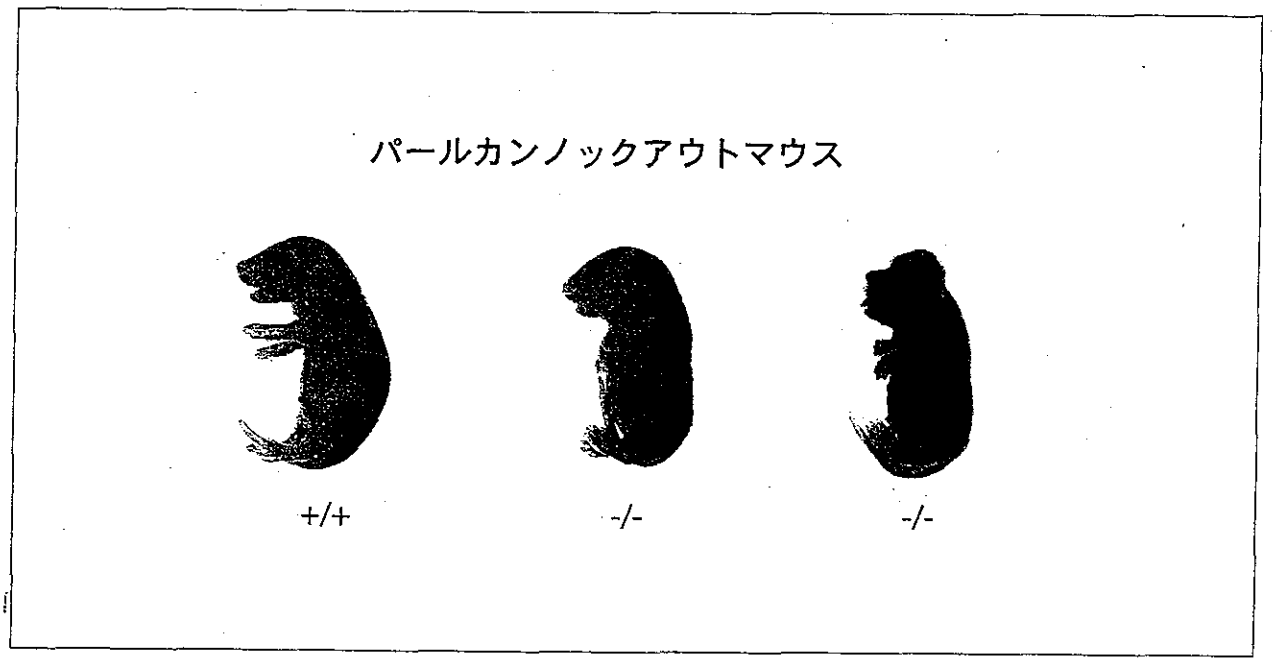

図2

により、二つの疾患における予後の違いはDDSH変異を持つパールカンは細胞外へ分泌されず、SJS変異を持つパールカンは細胞外に分泌され細胞外マトリックスとして部分的に機能するという違いによることが解った。細胞外にパールカンが分泌されるか否かは遺伝子変異の種類と位置にもより、構造変化や分泌シグナルを含めた検討が必要と考えられる。

神経筋接合部におけるパールカンの特異的機能の解明にむけて

さて、予後良好なSJS患者でも骨格異常を呈し、このことはパールカン欠損により説明されるが、ミオトニア症状の発症機序は非常に興味深いと思われる。ミオトニアとは筋の弛緩障害である。パールカンは筋組織においても基底膜の重要な構成成分であるが、発生が成熟するに従い神経筋接合部に多く存在してくる。神経筋接合部においては、アセチルコリン(ACh)とニコチン型ACh受容体の結合が後シナプス膜の脱分極を引き起こし筋が収縮する。筋の収縮と弛緩を速やかに制御するため、ここにはACh受容体やアセチルコリンエステラーゼ(AChE)をはじめとする多くの分子が集合し共同して働く必要がある（図3）。AChEはAChを加水分解することによりこの反応を収束させるとともに、AChのリサイクルに貢献する酵素である。神経筋接合部ではコラーゲン様の分子（collagen-like tail subunit; ColQ）ドメインをもつ基底膜特異的なAChEが存在するが[12]、*in vitro*の実験結果からこの分子がパールカンと結合することが想定されていた[13]。パールカンノックアウトマウスは周産期に死亡するが、筋の発生、分化、神経支配、神経筋接合部形成は少なくともこの時期まではほぼ正常に達成されていた。ところが、ACh受容体、アグリン、ラプシン、αジストログリカンといった神経筋接合部集合分子の集積に異常がないのに、AChEのみが特異的に欠損していることが解った[14]。ノックアウトマウス筋全体の生化学的解析ではColQ フォームを含めたすべてのAChEが発現していることから、産

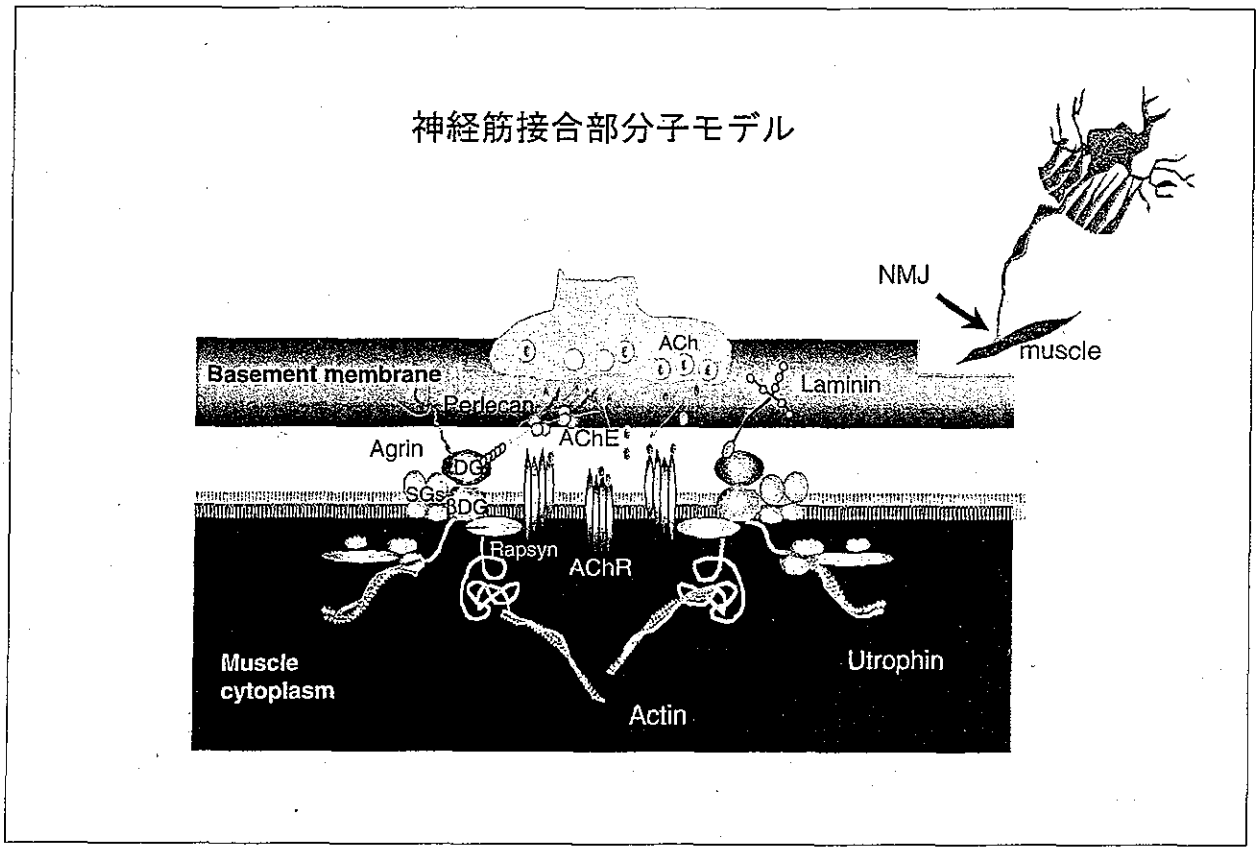

図3

生されたColQフォームが神経筋接合部に局在化することの障害によると考えられる。この結果はAChEの神経筋接合部への局在にパールカンが必須の働きをすることを示唆している。*In vitro* の実験系ではColQ分子がヘパラン硫酸鎖と結合するとされているが、神経筋接合部形成のキー分子とされるヘパラン硫酸プロテオグリカン；アグリンではAChEの局在が代償できないことは糖鎖の特異性を示唆する結果である。これらの結果がSJSにおける筋のミオトニア症状（弛緩障害、持続収縮）と関連するのか興味深く、新しいモデルマウスを使った電気生理学的解明や治療実験を検討中である。

おわりに

基底膜型プロテオグリカンであるパールカンはノックアウトマウスやヒト遺伝性疾患での解析結果から、基底膜構成成分としては必須ではなくむしろ機能分子として重要かつ多彩な働きをもつことが解ってきた。プロテオグリカンのコア蛋白質の特異性と糖鎖の組み合わせ、あるいは糖鎖そのものの多様性にますます面白い研究展開が予想される。

参考文献

1. Iozzo, R.V. Perlecan: a gem of a proteoglycan. *Matrix Biol* **14**, 203-8. (1994).
2. Iozzo, R.V., Cohen, I.R., Grassel, S. & Murdoch, A.D. The biology of perlecan: the multifaceted heparan sulphate proteoglycan of basement membranes and pericellular matrices. *Biochem J* **302**, 625-39. (1994).
3. Iozzo, R.V. et al. Structural and functional characterization of the human perlecan gene promoter. Transcriptional activation by transforming growth factor-beta via a nuclear factor 1-binding element. *J Biol Chem* **272**, 5219-28. (1997).
4. Jiang, X. & Couchman, J.R. Perlecan and tumor angiogenesis. *J Histochem Cytochem* **51**, 1393-410 (2003).
5. Arikawa-Hirasawa, E., Watanabe, H., Takami, H., Hassell, J.R. & Yamada, Y. Perlecan is essential for cartilage and cephalic development. *Nat Genet* **23**, 354-8 (1999).
6. Costell, M. et al. Perlecan maintains the integrity of cartilage and some basement membranes. *J Cell Biol* **147**, 1109-22 (1999).
7. Arikawa-Hirasawa, E. et al. Dyssegmental dysplasia, Silverman-Handmaker type, is caused by functional null mutations of the perlecan gene. *Nat Genet* **27**, 431-4. (2001).
8. Arikawa-Hirasawa, E. et al. Structural and functional mutations of the perlecan gene cause Schwartz-Jampel syndrome, with myotonic myopathy and chondrodysplasia. *Am J Hum Genet* **70**, 1368-75 (2002).
9. Arikawa-Hirasawa, E., Wilcox, W.R. & Yamada, Y. Dyssegmental dysplasia, Silverman-Handmaker type: unexpected role of perlecan in cartilage development. *Am J Med Genet* **106**, 254-7 (2001).
10. Hassell, J., Yamada, Y. & Arikawa-Hirasawa,

Point:
パールカンの機能解明から、ヘパラン硫酸プロテオグリカンの機能の多様性が示されました。さらに糖鎖機能の多様性が解明されることが期待されます。また、このような多様性を解明する場合、総合的結果として生体はどのような異常を呈するのかを動物モデルで検討することが疾患との関連で重要であることが示唆されました。

Key word:
パールカン、ヘパラン硫酸プロテオグリカン、細胞外マトリックス、軟骨異栄養症、ノックアウトマウス、神経筋接合部、ミオトニア

E. Role of perlecan in skeletal development and diseases. *Glycoconj J* **19**, 263-7 (2002).
11. Nicole, S. et al. Perlecan, the major proteoglycan of basement membranes, is altered in patients with Schwartz-Jampel syndrome(chondrodystrophic myotonia). *Nature Genetics* **26**, 480-483 (2000).
12. Krejci, E., Legay, C., Thomine, S., Sketelj, J. & Massouile, J. Differences in expression of acetylcholinesterase and collagen Q control the distribution and oligomerization of the collagen-tailed forms in fast and slow muscles. *J Neurosci* **19**, 10672-9 (1999).
13. Peng, H.B., Xie, H., Rossi, S.G. & Rotundo, R.L. Acetylcholinesterase clustering at the neuromuscular junction involves perlecan and dystroglycan. *J Cell Biol* **145**, 911-21 (1999).
14. Arikawa-Hirasawa, E., Rossi, S.G., Rotundo, R.L. & Yamada, Y. Absence of acetylcholinesterase at the neuromuscular junctions of perlecan-null mice. *Nat Neurosci* **5**, 119-23 (2002).

Profile

順天堂大学医学部卒。神経内科専攻。現在神経、筋における細胞外マトリックスの役割について *in vivo*,*in vitro*の両方の系を使って解明していきたいと思います。
発生や疾患との関連を明らかにし、基礎研究と臨床の現場の連携を目指します。